Nicotine-induced brain stimulation reward is modulated by melanocortin-4 receptors in ovariectomized rats

Manoj A. Upadhya [a,b,1,2], Harshita M. Upadhya [b,1], Chandrashekhar D. Borkar [b,3], Amit G. Choudhary [a,b], Uday Singh [c,4], Priyanka Chavan [d], Amul Sakharkar [d], Praful Singru [c], Nishikant K. Subhedar [a], Dadasaheb M. Kokare [b]*

Running title: Importance of MC4-Rs in nicotine reward in OVX rats

[a] Indian Institute of Science Education and Research (IISER), Dr. Homi Bhabha Road, Pashan, Pune- 411 008, Maharashtra, India

[b] Department of Pharmaceutical Sciences, Rashtrasant Tukadoji Maharaj Nagpur University, Nagpur- 440 033, India

[c] School of Biological Sciences, National Institute of Science Education and Research (NISER), Bhubaneswar, Jatni, Odisha 752 050, India

[d] Department of Biotechnology, Savitribai Phule Pune University, Pune- 411 007, India

[1] *Both the authors contributed equally*

Present Address:

[2] Neuroscience and Pharmacy Department, School of Life & Health Sciences, Aston University, B47ET, Birmingham, UK

[3] Department of Psychology (Brain Institute), School of Science and Engineering, Tulane University, New Orleans- 70118, LA, USA

[4] Department of Pharmacology, University of Iowa Carver College of Medicine, Iowa City, USA

Number of Pages: 32
Number of Figures: 08
Number of Supplementary Tables: 03

*** Corresponding Author:**
Dr. Dadasaheb M. Kokare
Department of Pharmaceutical Sciences,
Rashtrasant Tukadoji Maharaj Nagpur University,
Amravati Road,
Nagpur, Maharashtra, 440 033, India
Tel.: +91-9850318502
Fax: +91-712-2500355
E-mail: kokaredada@yahoo.com

ABSTRACT:

Apart from reproduction, estrogen influences a multitude of processes. Increase in estrogen levels in women is known to promote reward probably mediated via the melanocortin and dopamine systems. Reduced estrogen in post-menopausal women attenuates reward evoking the need for stimulation with greater rewarding salience. This is reflected in the well-recognized phenomena of difficulty in quitting and increased craving for nicotine in women following the onset of menopause. The present study aims at understanding the role of melanocortin receptors (MC-R) in nicotine-induced reward behavior following ovariectomy in rats. The MC4-R mRNA level was increased in ipsilateral nucleus accumbens (Acb) of the intact rats implanted with electrode in medial forebrain bundle and trained in intracranial self-stimulation (ICSS) paradigm. Additional groups of ICSS trained rats were ovariectomized (OVX) and subjected to reward evaluation. Trained OVX rats revealed a significant increase in threshold frequency and rightward shift in rate frequency curve, suggesting reward deficit behavior. However, pre-administration with nicotine, α-MSH or NDP-MSH (MC4-R agonist) to OVX animals restored the rewarding activity in ICSS protocol; HS014 (MC4-R antagonist) suppressed the lever press activity. Prior treatment with sub-effective doses of α-MSH or NDP-MSH potentiated the reward effect of nicotine, but was attenuated by HS014. Alpha-MSH-immunoreactivity was decreased in the Acb shell, arcuate and paraventricular nucleus of hypothalamus, and ventral bed nucleus of stria terminalis in the OVX rats, while nicotine treatment restored the same. We suggest a role for the endogenous MC system, perhaps acting via MC4-R, in the nicotine-induced reward in OVX rats.

Keywords: Nicotine; Melanocortin receptors; Ovariectomy; Brain stimulation reward; qRT-PCR; Immunofluorescence

INTRODUCTION

Menopausal anhedonia is a serious problem in aging women. Loss of ovarian hormones is believed to suppress the reward processing mechanisms driving the subjects to drugs. While elevated estradiol titer is associated with an increased likelihood of quitting regular smoking (Peltier et al., 2019), women lacking estrogen face difficulty in giving up nicotine and are prone to increased risk of coronary vascular disease (Lee and Cooke, 2011), lung carcinogenesis (Wassenaar et al., 2013), acute glomerulonephritis and ureteral obstruction (Jaimes et al., 2009). Estradiol is known to alter dopamine activity in female rats (Flores et al., 2016). Russo et al. (2003) reported decrease in dopamine level in ventral tegmental area (VTA) in ovariectomized (OVX) animals (a model of menopausal condition). Brain stimulation reward (BSR) is diminished in the OVX rats, although the effect was reversed by estradiol (Galankin et al., 2010). VTA, the primary centre of the mesolimbic reward system, is also a well recognized target for nicotine. Nicotine stimulates nicotinic acetylcholine receptors (nAChRs) at different nodes of the reward pathway including VTA and nucleus accumbens (Acb) (Laviolette and Van der Kooy, 2004). *In vivo* microdialysis studies suggest that systemic nicotine increases dopamine release in the Acb by enhancing the excitatory input to the VTA via local α7 nAChRs (Schilstrom et al., 1998). In addition, Tapinc and colleagues (2017) reported that subcutaneous nicotine treatment upregulated the pro-opiomelanocortin (POMC) mRNA in the hypothalamus, melanocortin 4-receptors (MC4-R) mRNA in the medial prefrontal cortex and increased MC3-R mRNA expression in the VTA. Intraperitoneal (ip) nicotine treatment decreased alpha-melanocyte stimulating hormone (α-MSH) levels in rat plasma (Conte-Devolx et al., 1981). Isolated perfused mouse brain and frog neuro-intermediate lobe showed increased α-MSH secretion following nicotine treatment (Marty et al., 1985; Garnier et al., 1994). In contrast to these findings, Qi et al. (2015) reported that MC4-R do not play a role in the dysphoria associated with nicotine withdrawal. Although the literature suggests wide range of interaction between nicotine and MC, contribution of MCs in nicotine-mediated reward behavior is not studied till date. Moreover, how nicotine induced reward behaviour is mediated in the absence of estradiol also remains a topic

of high value. Therefore, we wanted to investigate the role of MCs in the susceptibility of post-menopausal females to nicotine addiction.

We studied the dose-dependent effect of nicotine in intact as well as OVX rats on intracranial self-stimulation (ICSS) behaviour in operant conditioning chamber. Further, the dose-dependent effect of α-MSH, NDP-MSH (non-selective MC3- and MC4-R agonist) or HS014 (selective MC4-R antagonist) in OVX rats was also investigated in ICSS protocol. To investigate the role of MC system in rewarding action of nicotine, α-MSH, NDP-MSH or HS014 was administered prior to nicotine and rats were subjected to ICSS. Since, the MC4-R in Acb are also known to mediate reward (Hsu et al., 2005), we studied MC4-R gene expression in contralateral and ipsilateral part of Acb using qRT-PCR in unconditioned and conditioned rats. The effect of nicotine on endogenous α-MSH system was investigated in the naïve, unconditioned OVX and, conditioned as well as OVX rats using immunofluorescence method. Herein, the response of the cells in the arcuate nucleus of hypothalamus (ARC), along with fibre terminals in the Acb shell (AcbSh), paraventricular nucleus of hypothalamus (PVN), lateral part of bed nucleus of stria terminalis (BNSTl) and central nucleus of amygdala (CeA) was evaluated. These regions are reported to be involved in the processing of reward related information in the brain (Desai et al., 2013; Koob, 2000; Ahmed et al., 2005).

MATERIALS AND METHODS

Experimental animals

Adult female Sprague-Dawley rats weighing 220-260 g were group housed in polypropylene cages at temperature 25 ± 1 °C and 12:12 h light/dark cycle, light on at 0700 h. However, after electrode implantation and/or intracerebroventricular (icv) cannulation and during experiments, the animals were housed individually. They had free access to rodent laboratory chow food (Trimurti Feeds, Nagpur, India) and tap water. The behavioral assessment was undertaken during the light cycle between 0900 to 1400 h. All experimental protocols were approved by the Institutional Animal Ethics Committee of Department of Pharmaceutical Sciences, Rashtrasant Tukadoji Maharaj Nagpur University, Nagpur, India.

Surgery for intracerebroventricular (icv) cannulation and intra-medial forebrain bundle (MFB) electrode implantation

All rats were first cannulated for electrode implantation targeted at medial forebrain bundle (MFB) and guide cannula was placed in lateral ventricle. The details of these procedures and post-surgical care have been standardized in our laboratory (Upadhya et al., 2012; Somalwar et al., 2017). Briefly, rats were weighed and anaesthetized with thiopentone sodium (45 mg/kg, ip, Abbott Pharmaceuticals, Mumbai, India). Following hair depilation, each rat was placed in a stereotaxic instrument (David Kopf Instruments, USA), a mid-sagittal dorsal skull incision was made through the skin, the underlying fascia cleared and a hole was drilled through the skull over coordinates corresponding to the site of interest. The stereotaxic coordinates -0.8 mm posterior, +1.3 mm lateral to midline and -3.5 mm ventral from skull surface for guide cannula implantation into the right lateral ventricle and -2.8 mm posterior, -1.7 mm lateral to midline and -8.5 mm ventral for implantation of bipolar electrode into the MFB was selected (Paxinos and Watson, 1998). Guide cannula and electrode were secured to the skull using 1 mm screws and a flush-fitting stylet was inserted into the guide cannula to prevent blockage (Kokare et al., 2011). The rats were allowed to recover for 7 days following surgery. During this period the animals were handled daily and their behavior was recorded for motor disturbances, if any. The food and water was available *ad libitum*.

Habituation to the animals

One week after surgery, the rats were divided into separate groups (n = 6-8/group), and habituated to the testing environment, transferring to experimental room. Animals were handled twice daily, the procedure consists of weighing the animals and manually restraining them on platform for 1 min with gently removing and replacing the stylet, the same platform was used during drug administration.

Conditioning of rats for electrical self-stimulation

Following post-surgical period, animals were conditioned for the reward in the ICSS chamber (Coulbourn Instruments, USA, 30.48 x 25.4 x 30.48 cm). The procedure has been standardized and routinely followed in our laboratory (Desai et al., 2013;

Somalwar et al., 2017). Briefly, the rats implanted with stimulating electrode targeted at the LH-MFB area were individually trained in an operant chamber on a continuous reinforcement schedule fixed ratio 1 (FR1) to press the lever for electrical self-stimulation. The stimulator (Coulbourn Instruments, USA) was connected to the electrodes *via* stimulating cable (Desai et al., 2014) and was controlled by software (Graphic State Notation-3.03).

ICSS procedure

A rate-frequency curve-shift method was employed (Miliaressis et al.,1982; Coulombe and Miliaressis, 1987; Carlezon and Chartoff, 2007; Somalwar et al., 2017) to determine ICSS thresholds. Each active lever press by the animal illuminated the cue light and delivered a 0.5 sec train of square-wave cathodal pulses (0.1 msec pulse duration) at a defined frequency of 186 Hz [log(2.270)]. During the training session, the stimulation current in the range of 100-300 µA was gradually adjusted for each rat such that the lowest value applied would produce a constant rate of lever pressing. Animals showing the maximal rates of 35-40 lever press/min were selected for the behavioral assay. The animals showing lever press activity less than that were excluded. During the behavioral assay, the current intensity in the narrow range of 200-225 µA was employed and each rat was subjected to fifteen trials of descending series of frequencies (often called as a 'pass') of one min duration each for one or two weeks. One min frequency trial comprised of 5 sec priming phase, 50 sec test phase and 5 sec time-out phase, where each phase delivered electrical pulses for 500 msec followed by 500 msec time-out (no stimulation). During initial 5 sec priming phase, five non-contingent stimulations were delivered. Following the primes, there was a 50 sec test phase in which the number of lever pressings were recorded. The stimulation frequency was then reduced by about 10% (0.05 $\log_{10}$ units) and another trial (pass) was initiated. After each stimulation phase, a 500 msec time-out period was allowed during which no stimulation is earned even if the animal presses the lever. Once the 50 sec test period is complete, there is a 5 sec time-out period during which no stimulation is available, and this completes 60 sec trial. The stimulation frequency was then reduced by 10% (about 0.05 $\log_{10}$ units) and another trial was initiated.

The ICSS threshold (M_{50} and T_0) was calculated using nonlinear regression curve fit method by Graphpad Prism 5 software, as a measure of reward and

reinforcement (Miliaressis et al., 1982; Coulombe and Miliaressis, 1987; Somalwar et al., 2017). While M_{50} value or 'half maximum' denotes the frequency that maintains 50% of maximal responding, 'Theta-0' (T_0) (rate of responding > 0) indicate the frequency at which the stimulation becomes rewarding and where the line intersects the x-axis. The leftward shift in the rate-frequency curve function indicated reward facilitation, while the rightward shift suggested reward attenuation (Wise, 1996; Carlezon and Chartoff, 2007). As soon as mean thresholds stabilized (< 10% variation), the effect of nicotine, α-MSH, NDP-MSH, HS014 and combination thereof on reward thresholds was investigated. On each test day, three rate-frequency curves were generated for each animal, immediately prior to the drug treatment. In the case of each treated animal, three additional trials of 15 min rate-frequency curve were conducted. However, the naïve animals (unconditioned) underwent surgical procedure for implantation of electrode at LH-MFB area, but they were not subjected to ICSS conditioning.

Reverse transcriptase-quantitative PCR (qRT-PCR) for MC4-R mRNA measurements

With a view to determine the effect of ICSS conditioning on MC4-R mRNA, brains were removed from a unconditioned and ICSS conditioned rats, snap frozen using dry ice and stored at -80° C. These brains were sectioned and the Acb tissues from ipsilateral and contralateral hemispheres were punched out from the bregma-matched brain slices as shown in the Fig. 1C). The qRT-PCR was employed to study the effect of ICSS conditioning on expression of MC4-R mRNA in the Acb. The total cellular RNA was isolated by TRIZOL (Ambion, Carlsbad, CA, USA) method as per manufacturer's instructions. For the removal of DNA contamination from the total RNA preparation, DNase I enzyme (Invitrogen, Carlsbad, CA, USA) was used. Further the DNase was heat inactivated and the quality and quantity of RNA was estimated by Biospec Nano Micro-volume UV-Vis Spectrophotometer (Shimadzu, Kyoto, Japan). The RNA was reverse transcribed using random hexamers and iScript cDNA synthesis kit (Bio-Rad, CA, USA) in a final volume of 10 µL, according to the manufacturer's instructions. The PCR conditions used for the reverse transcription were as follows: 25°C for 5 minutes; 45°C for 20 min; 95°C for 1 min. The cDNA was then subjected to

qRT-PCR with SYBR green qPCR master mix (Bio-Rad, CA, USA) and 50 pmol of specific primers on CFX96^{TM} Real time-PCR System (Bio-Rad Laboratories, CA, USA). All the reactions were performed in duplicates. The thermal profile used for the reaction is, 95°C for 10 min followed by 40 cycles of 95°C for 15 sec, 60°C for 15 sec. Further melt curve analysis was performed in the temperature range of 65ºC to 95°C with 0.5°C increment at a rate of 5 sec/step. MC4-R primer sequence used in this study is given below, F5'-GGGTGTCATAAGCCTGTTGGA-3'and R5'-GCCACAGCCACTACAGAT-3'. The β- actin gene was used as an internal control and the data normalization was conducted as described previously by Sagarkar et al. (2017), using $2^{-\Delta\Delta CT}$ method (Livak and Schmittgen, 2001).

Ovariectomy in rats

Rats were cannulated targeting MFB electrode and trained in operant chamber for self-stimulation as mentioned above. Once the stable lever pressings for self-stimulation were obtained, the rats were subjected to ovariectomy surgery under thiopentone sodium (45 mg/kg, ip) anesthesia. Approximately 2 cm incision was made through the lower abdominal skin, fallopian tubes were traced and both ovaries were removed. The inner skin was sutured with interrupted absorbable sutures (TRUGUT®, 5-0). The outer skin was sutured with sterilized silk threads (4-0) and the animals were transferred to their home cage.

Drug administration and evaluation in operant conditioning chamber

All drugs used in the study were purchased from Sigma, St. Louis, MO. The details on the agents/drugs and the dosages are summarized in Suppl Table 1. The doses were selected based upon earlier studies (Torres et al., 2009; Shelkar et al., 2015) and a separate dose-response study was undertaken. Nicotine (Nicotine hydrogen tartarate; Catalogue No. SML1236) was freshly prepared by dissolving in saline and given as a single dose to ICSS trained non-OVX and OVX rats via intraperitoneal (ip) route. Then the rats were tested for lever press activity. The doses of nicotine used in the present study represent the free base nicotine and were calculated from the hydrogen tartarate salt. Melanocortin agonists (α-MSH and NDP-MSH) or selective MC4-R antagonist (HS014) were dissolved in artificial cerebrospinal

fluid (aCSF) and injected into the right lateral ventricle in ICSS trained OVX rats. In dose dependent study, each rat received two injections (saline + saline or nicotine, or aCSF + the aCSF or melanocortin agents) separated by an interval of 15 min. In combination study, melanocortin agonists/ antagonists + nicotine were given 15 min apart. Fifteen min after the second injection, each animal was subjected to ICSS test in operant conditioning chamber. These animals were also tested for the locomotor activity in open field and the numbers of crossovers were recorded.

Verification of guide cannula and electrode placement

At the end of each experiment, dilute India ink was injected by icv route and animals were euthanized by an overdose of thiopental sodium (65 mg/kg, ip). The brains were dissected out and cut in coronal plane to verify the placement of the guide cannula and distribution of ink in the ventricles. The data drawn from the animals that showed correct placement of the cannula and uniform distribution of ink in the ventricles were considered. Similarly, for verification of electrode in MFB, the brains were removed, sectioned and the position of the tip of each electrode site was determined (Fig. 1A and B).

Immunofluorescence and morphometric analysis

Different groups of naïve (unconditioned), OVX (unconditioned) and ICSS trained rats (n = 5 /group) were used in the immunofluorescence study. The rats trained for self-stimulation were divided into the following groups 1) trained for self-stimulation and treated with single injection of saline or nicotine (1 mg/kg, ip); 2) trained for self-stimulation, subjected to ovariectomy and treated with single injection of saline or nicotine (1 mg/kg, ip). Thirty minutes after the saline or nicotine injection, the rats were anesthetized (thiopental sodium, 65 mg/kg, ip), perfused transcardially with ice-cold heparinized phosphate-buffered saline (PBS; pH 7.4) for 30 sec followed by 4% paraformaldehyde in 0.1 M phosphate buffer (pH 7.4) for 10-15 min. The brains were post-fixed in the same fixative overnight, cryoprotected in 30% sucrose solution in PBS, embedded, and serially sectioned on a cryostat (Leica, Germany) at 30 µm thickness in the coronal plane and collected in PBS.

Sections were then processed for α-MSH-immunolabeling using immunofluorescence method described earlier (Kokare et al., 2010; Shelkar et al., 2015). The sheep polyclonal α-MSH antiserum was used in the present study (a generous gift from Professor Jeffrey Tatro, Tufts Medical Center, Boston, MA, USA). Briefly, the sections were incubated in sheep antibodies against α-MSH diluted in PBS (1:10,000) containing 2% normal horse serum, 0.3% Triton X-100, 0.2% Kodak PhotoFlo solution and 0.08% sodium azide for 48 h at 4 ºC. Sections were washed in PBS and incubated in DyLight 488-conjugated anti-sheep IgG (Jackson Immunoresearch, West Groove, PA, USA) at 1:250 dilution for 4 h at room temperature, again washed in PBS and cover slipped with propyl gallate mounting medium. Sections were observed with 20X/0.50 objective under Leica DM2500 fluorescence microscope using a filter set 488 for DyLight. Desired areas were captured using Leica DFC450 C camera, adjusted for brightness and contrast, and merged using Adobe Photoshop CS4 software. Brain sections of different groups were concurrently processed under identical conditions to ensure reliable comparisons among different groups and maintain stringency in tissue preparation and staining conditions.

Specificity of the α-MSH antiserum

The polyclonal sheep α-MSH antiserum has been widely used for the localization of α-MSH in the rat brain (Elias et al., 1998a; Fekete et al., 2000; Singru et al., 2005; Kokare et al., 2010; Shelkar et al., 2015). The antiserum was raised against α-MSH peptide conjugated to bovine thyroglobulin (Elias et al., 1998b). Specificity of this antiserum has been established by radioimmunoassay by using I-α-MSH as described earlier (Elias et al., 1998b). The application of preadsorbed α-MSH antiserum with excess α-MSH peptide completely blocked the immunostaining in the cells of the intermediate lobe of rat pituitary (Elias et al., 1998b). To further confirm the specificity of this antiserum, preadsorption procedure was employed. The sheep α-MSH antiserum was incubated with α-MSH peptide at 10^{-5} M for 24 h before incubation. Rat brain sections through the hypothalamus were incubated with either diluted α-MSH antiserum (1:10,000) or the preadsorbed antiserum and processed for immunofluorescence as described above. While several intensely labeled α-MSH cell bodies and fibers were seen in the ARC

following the application of anti-α-MSH antiserum (Fig. 1Ei), no immunoreactivity was seen in the sections incubated with the preadsorbed antiserum (Fig. 1Eii).

Morphometric analysis

The optical density per unit area (μm^2) covered by α-MSH-immunoreactivity was estimated from the transverse sections passing through the AcbSh, ARC, BNSTl, PVN and CeA from the naïve control, trained intact and OVX (saline and nicotine treated) using microscopic images from predetermined areas in the sections. The images (X480) were analyzed using ImageJ software. The images of α-MSH-ir area were digitized, the background was considered as threshold, and integrated density occupied by immunostained cells/fibers were measured based on individual pixel intensity in all the control and treatment rats. Five measurements were taken from predetermined fields for each sub-region on ipsilateral side of each brain. The data for each nuclear group or area, from all animals in each group were pooled and the mean ± standard error of mean (SEM) was calculated. The skilled observer, blind to the treatments given, recorded the behavioral as well as morphometric measurements.

Statistical analysis

Data obtained from the behavioral studies were separately pooled, averaged and represented as mean ± standard error of mean (SEM). The rate-frequency curves were represented by curve fit method and statistically analyzed by two-way ANOVA with 95% confidence level, using GraphPad Prism 8.1.0 software. The ICSS threshold (M_{50} and T_0) was calculated using nonlinear regression curve fit method and analyzed using one-way ANOVA followed by post-hoc Bonferroni's multiple comparison test. Moreover, the data obtained from qRT-PCR and immunohistochemistry experiments were analyzed using t-test and one-way ANOVA followed by post-hoc Bonferroni's multiple comparisons test, respectively. Differences were considered significant at $p < 0.05$.

RESULTS

Effect of ICSS on MC4-R gene expression in the nucleus accumbens

The mRNA levels of MC4-R in the Acb on ipsilateral and contralateral sides of the conditioned and the unconditioned rats were estimated using qRT-PCR. The

electrical self-stimulation in the LH-MFB significantly ($p < 0.05$) increased the MC4-R mRNA expression in the Acb of conditioned rats in ipsilateral side as compared to that in the unconditioned rats. On the other hand, MC4-R mRNA expression in the Acb on the contralateral side to the ICSS in conditioned rats showed significant decrease ($p < 0.05$) as compared to that in the unconditioned controls (Fig. 1D). We suggest that the increase in the MC4-R mRNA expression may be a consequence of ICSS conditioning.

Self-stimulatory activity in OVX rats using the operant chamber

In the operant chamber, the number of lever press was counted in the intact (naive) and sham-OVX animals conditioned to ICSS. Both the groups showed decremental lever press activity following the application of decreasing series of frequency. In comparison, the trained OVX rats showed reduction in lever press activity [factor 'frequency' $F_{(15,240)} = 268.3$, $p < 0.0001$; factor 'treatments' $F_{(2,240)} = 99.87$, $p < 0.0001$ and interaction 'treatment' x 'frequency' $F_{(30,240)} = 4.851$, $p < 0.0001$] (Fig. 2A). The rightward shift was noticed in the rate frequency curve in these rats as compared to those in the intact or sham-OVX rats. In addition, there was significant increase in the M_{50} [$F_{(2,17)} = 5.769$, $p < 0.05$] and T_0 [$F_{(2,17)} = 19.59$, $p < 0.001$] in OVX rats as compared to that in the intact or sham-OVX animals (Fig. 2B and C).

Nicotine dose-dependently facilitates ICSS activity in intact and OVX rats

The rate of lever pressings in intact rats trained in the operant chamber was increased significantly following the nicotine (0.1-0.5 mg/kg, ip) treatment. The frequency-response curve was also shifted towards the left [factor 'frequency' $F_{(15,256)} = 448.2$, $p < 0.0001$; factor 'treatments' $F_{(3,256)} = 213.3$, $p < 0.0001$ and interaction 'treatment' x 'frequency' $F_{(45,256)} = 5.807$, $p < 0.0001$], reflecting the reward effect of nicotine in ICSS paradigm (Fig. 2D). Moreover, nicotine treatment significantly decreased the M_{50} value [$F_{(3,19)} = 9.991$, $p < 0.001$] at 0.3 and 0.5 mg/kg doses and T_0 value [$F_{(3,19)} = 3.576$, $p < 0.05$] at 0.5 mg/kg as compared to saline treated controls (Fig. 2E and F).

Similarly, single injection of nicotine (0.5-1 mg/kg, ip) in OVX rats significantly increased contingent lever pressings in a dose-dependent manner. The leftward shift in the frequency-response curve suggests the rewarding effect of nicotine [factor 'frequency' $F_{(15,527)} = 348.1$, $p < 0.0001$; factor 'treatments' $F_{(4,527)} = 333.0$, $p < 0.0001$ and interaction 'treatment' x 'frequency' $F_{(60,527)} = 10.33$, $p < 0.0001$] (Fig. 2G). A significant decrease in M_{50} [$F_{(4,37)} = 5.259$, $p < 0.01$] and T_0 [$F_{(4,37)} = 11.72$, $p < 0.0001$] was observed following nicotine treatment. Post-hoc Bonferroni's multiple comparisons test revealed that nicotine produced significant potentiation of reward (decrease in M_{50} and T_0) compared to saline treatment at 0.5 and 1 mg/kg dose of nicotine (M_{50} at 1 mg/kg, $p < 0.05$; T_0 at 0.5 mg/kg, $p < 0.05$ and at 1 mg/kg, $p < 0.001$). On the other hand, the lower dose of nicotine (0.3 mg/kg, ip) did not affect M_{50} and T_0 values significantly ($p > 0.05$) and therefore considered as sub-effective (Fig. 2H and I). Thus, nicotine treatment at 0.5 and 1 mg/kg dose seems to promote rewarding behavior in the OVX rats.

α-MSH dose-dependently facilitates ICSS activity in OVX rats

α-MSH microinjections (0.5-1.5 µg/rat) in the lateral ventricle in OVX rats dose-dependently increased the number of lever pressings and lowered ICSS threshold as indicated by leftward shift in rate-frequency curve [factor 'frequency' $F_{(15,496)} = 343.7$, $p < 0.0001$; factor 'treatments' $F_{(4,496)} = 184.7$, $p < 0.0001$ and interaction 'treatment' x 'frequency' $F_{(60,496)} = 6.583$, $p < 0.0001$] (Fig. 3A). A significant decrease in M_{50} [$F_{(4,34)} = 4.472$, $p < 0.01$] and T_0 [$F_{(4,34)} = 11.49$, $p < 0.0001$] was also observed following α-MSH treatment. One way ANOVA and post-hoc Bonferroni's multiple comparisons test revealed that α-MSH produced significant decrease in M_{50} (at 1.5 µg/rat, $p < 0.05$) and T_0 (at 1.0 µg/rat, $p < 0.05$ and at 1.5 µg/rat, $p < 0.001$) compared to that in the aCSF control (Fig. 3B and C). On the other hand, at lower dose (0.5 µg/rat), α-MSH failed to influence the number of lever pressings or the reward thresholds and therefore considered sub-effective (M_{50} and T_0, $p > 0.05$).

NDP-MSH dose-dependently promotes self-stimulatory activity in OVX rats

Fig. 3D depicts the frequency-response curve obtained from the rats before and after aCSF and NDP-MSH injections in OVX rats. Application of two-way ANOVA showed a significant increase in lever press activity in NDP-MSH (0.2 and 0.4 µg/rat) treated animals; the treatment shifted the curves towards the lower frequencies, reflecting increased reward [factor 'frequency' $F_{(15,448)} = 375.7$, $p < 0.0001$; factor 'treatments' $F_{(4,448)} = 347.0$, $p < 0.0001$ and interaction 'treatment' x 'frequency' $F_{(60,448)} = 12.50$, $p < 0.0001$]. While one-way ANOVA treatment of the data showed a significant effect of dose for M_{50} [$F_{(4,32)} = 10.10$, $p < 0.001$] and T_0 [$F_{(4,32)} = 8.33$, $p < 0.001$], post-hoc Bonferroni's multiple comparisons test revealed that NDP-MSH treatment at 0.4 µg/rat decreased M_{50} ($p < 0.01$) and T_0 ($p < 0.01$) as compared to that in the aCSF treated rats. This suggested significant potentiation of reward by NDP-MSH. However, NDP-MSH at lower doses (0.1 and 0.2 µg/rat) failed to reduce the M_{50} and T_0 values and therefore considered as sub-effective (Fig. 3E and F).

HS014 dose-dependently inhibits self-stimulatory activity in OVX rats

Icv administration of HS014 (0.1 and 0.2 µg/rat) in OVX rats attenuated the reward behavior in ICSS as depicted by shift of the rate-frequency curves towards right side [factor 'frequency' $F_{(15,448)} = 248.1$, $p < 0.0001$; factor 'treatments' $F_{(4,448)} = 43.99$, $p < 0.0001$ and interaction 'treatment' x 'frequency' $F_{(60,448)} = 3.884$, $p < 0.0001$] (Fig. 3G). Statistical analysis using one-way ANOVA revealed a significant effect of HS014 treatment on M_{50} [$F_{(4,32)} = 11.04$, $p < 0.001$] and T_0 [$F_{(4,32)} = 6.968$, $p < 0.001$]. Moreover, application of post-hoc Bonferroni's multiple comparisons test showed that HS014 significantly increased M_{50} (at 0.1 µg/rat, $p < 0.05$, at 0.2 µg/rat, $p < 0.001$) and T_0 (0.2 µg/rat, $p < 0.05$) as compared to aCSF, indicating attenuation of reward. However, at lower dose (0.05 µg/rat), HS014 failed to increase M_{50} and T_0 values and therefore considered as sub-effective (Fig. 3H and I).

α-MSH, NDP-MSH or HS014 modulates the effect of nicotine on ICSS activity in OVX rats

With a view test if the rewarding action of nicotine is via melanocortin system, we administered α-MSH at sub-effective dose (0.5 µg/rat) in combination with nicotine at sub-effective (0.3 µg/rat) or effective dose (0.5 µg/rat) and screened the ICSS activity.

Significant potentiation in the nicotine induced reward behavior in OVX rats was observed following combination treatments of sub-effective doses of both agents as well as sub-effective α-MSH + nicotine effective doses as compared to respective nicotine *per se* [factor 'frequency' $F_{(15,576)} = 542.1$, $p < 0.0001$; factor 'treatments' $F_{(5,576)} = 286.6$, $p < 0.0001$ and interaction 'treatment' x 'frequency' $F_{(75,576)} = 10.75$, $p < 0.0001$] (Fig. 4A). Application of one-way ANOVA showed significant elevation in M_{50} [$F_{(3,27)} = 6.229$, $p < 0.01$ and [$F_{(3,27)} = 6.017$, $p < 0.01$], and T_0 [$F_{(3,27)} = 14.99$, $p < 0.001$] and [$F_{(3,27)} = 29.60$, $p < 0.0001$] at α-MSH (0.5 µg/rat) + nicotine 0.3 and 0.5 mg/kg doses, respectively. Post-hoc Bonferroni's multiple comparisons test showed significant decrease in M50 in OVX rats treated with α-MSH prior to nicotine (for both combinations, $p < 0.05$) as compared to aCSF and nicotine (0.3 mg/kg) *per se*. Similarly, T_0 was also significantly reduced (for 0.5 µg/rat α-MSH + 0.3 mg/kg nicotine, $p < 0.05$; for 0.5 µg/rat α-MSH + 0.5 mg/kg nicotine, $p < 0.001$) as compared to aCSF (Fig. 4B and C).

NDP-MSH (0.1 µg/rat) administration by icv route, 15 min prior to nicotine (0.3 and 0.5 mg/kg, ip) increased the rate of lever presses and decreased reward thresholds as compared to that of the respective nicotine *per se* group [factor 'frequency' $F_{(15,608)} = 638.7$, $p < 0.0001$; factor 'treatments' $F_{(5,608)} = 215.3$, $p < 0.0001$ and interaction 'treatment' x 'frequency' $F_{(75,608)} = 9.774$, $p < 0.0001$] (Fig. 4D). A significant reduction in M_{50} [$F_{(3,28)} = 6.942$, $p < 0.01$ and [$F_{(3,28)} = 14.59$, $p < 0.001$] and T_0 [$F_{(3,28)} = 4.33$, $p < 0.05$ and [$F_{(3,28)} = 16.20$, $p < 0.0001$] was observed at NDP-MSH (0.1 µg/rat) + nicotine 0.3 and 0.5 mg/kg doses, respectively. Post-hoc Bonferroni's multiple comparisons test revealed the effect of treatment with sub-effective dose of NDP-MSH (0.1 µg/rat), prior to the sub-effective (0.3 mg/kg, ip) or effective dose (0.5 mg/kg, ip) of nicotine produced significant decrease in M_{50} (both $p < 0.05$) and T_0 (only at 0.5 mg/kg, ip; $p < 0.05$) as compared to nicotine *per se* (Fig. 4E and F).

To confirm the involvement of MC4-R in nicotine induced reward, sub-effective dose of HS014 (0.05 µg/rat) was given 15 mins prior to effective doses of nicotine (0.5 and 1 mg/kg, ip). HS014 treatment significantly suppressed the lever press activity of nicotine at 1 mg/kg, ip, as revealed by two-way ANOVA [factor 'frequency' $F_{(15,560)} = 553.4$, $p < 0.0001$; factor 'treatments' $F_{(5,560)} = 241.7$, $p < 0.0001$ and interaction

'treatment' x 'frequency' $F_{(75,560)} = 9.786$, $p < 0.0001$] (Fig. 4G). Application of one-way ANOVA showed significant elevation in M_{50} [$F_{(3,26)} = 13.48$, $p < 0.001$] and T_0 [$F_{(3,26)} = 32.57$, $p < 0.0001$] at HS014 (0.05 µg/rat) + nicotine 1 mg/kg doses, respectively (Fig. 4H and I). The rightward shift in rate-frequency curve suggested that nicotine-induced reward was attenuated by HS014 treatment, and the presence of HS014 prevented the drop in M_{50} and T_0 values produced by nicotine *per se*. However, HS014 treatment prior to 0.5 mg/kg nicotine did not show any attenuation in nicotine's effect. The raw values and conversion for obtaining T_0 and M_{50} are shown in Suppl Tables 2 and 3. None of the above treatments either *per se* or in combination produced any effect on the locomotor activity as compared to their respective control in open field test (data not shown).

Effect of nicotine treatment on α-MSH-immunoreactivity in trained and OVX rats

The nucleus accumbens shell (AcbSh)

Immunoreactive profile of α-MSH in the AcbSh of the various groups of rats is shown in Fig. 5 A1-A6 and Fig. 7A. While several α-MSH-ir fibers were seen in the AcbSh of naive control rats (A1), a significant decrease was observed in the OVX rats (A2, $p< 0.01$). Operant conditioning in the intact rats showed an increase in α-MSH-ir fiber density (A3, $p < 0.001$). On the other hand, the density of α-MSH-ir fibers in the AcbSh of the trained OVX rats was significantly decreased (A4, $p < 0.001$). The immunoreactivity in the nicotine treated intact rats (A5) was significantly higher ($p < 0.05$) as compared to that in the saline treated intact rats (A3). In addition, a highly significant increase was noticed in the OVX rats treated with nicotine (A6) as compared to that of the saline treated OVX rats (A4; $p < 0.001$). The morphometric analysis is represented in Fig. 7A.

The arcuate nucleus of hypothalamus (ARC)

The profiles of α-MSH-ir in different groups, and their morphometric analyses, are summarized in Figs. 5 B1-B6, 7 B and C. The α-MSH-ir density and cell count was significantly decreased ($p < 0.001$) in the OVX rats (B2) as compared to naïve (B1). On the other hand, highly significant increase in the density of α-MSH-ir cells and fibers,

and number of α-MSH positive cells was observed in intact conditioned, saline treated rats (B3; $p < 0.001$). The α-MSH-ir density and cell count in the ARC of the conditioned OVX rats was significantly decreased (B4; $p < 0.001$). In contrast, nicotine treatment in conditioned intact (B5; $p < 0.001$) as well as OVX (B6; $p < 0.001$) rats significantly increased the density of α-MSH-ir cells and fibers, and cell count as compared to their respective controls.

The bed nucleus of stria terminals, lateral division (BNSTl)

Fig. 5 C1-C6 shows several α-MSH-ir fibers in the BNSTl region. A dramatic decrease ($p < 0.001$) was observed in the α-MSH-ir fibers density in the OVX rats (C2) as compared to naïve control (C1). In contrast, significant increase in the density of α-MSH-ir fibers was observed in saline treated intact operant conditioned rats (C3; $p < 0.001$). The density of α-MSH-ir fibers in the BNSTl of the saline treated conditioned OVX rats was significantly decreased (C4; $p < 0.001$). On the other hand, nicotine treatment in conditioned OVX rats showed significant increase (C6; $p < 0.001$) as compared to that in the saline treated conditioned OVX rats (C4). The immunoreactive content in the BNSTl of intact nicotine treated conditioned rats (C5) was quite similar to that in the saline treated conditioned rats (C3; $p > 0.05$). The morphometric analyses of α-MSH-ir density in the BNSTl of the various groups of rats are summarized in Fig. 7 D.

The paraventricular nucleus of hypothalamus (PVN)

α-MSH-ir profile in the PVN of the various groups of rats, and their morphometric analyses are summarized in Figs. 6 A1-A6 and 7 E. While several α-MSH-ir fibers were seen in the PVN of naive control rats (A1), a significant decrease in the density was noted in OVX rats (A2, $p < 0.001$). On the other hand, the higher density of α-MSH-ir fibers was seen in saline treated operant conditioned rats (A3; $p < 0.001$). However, the density of α-MSH-ir fibers in the PVN of the conditioned OVX saline treated rats was significantly decreased (A4; $p < 0.001$). Nicotine treatment in conditioned intact (A5) and conditioned OVX (A6) rats significantly increased ($p < 0.001$) the density of α-MSH-ir fibers in PVN as compared to that in respective controls.

The central nucleus of amygdala (CeA)

Several α-MSH-ir fibers were seen in the CeA of naive control rats (Fig. 6 B1). The density of the α-MSH-ir fibers in CeA did not alter in OVX (B2; $p > 0.05$) and operant conditioned saline treated rats (B3; $p > 0.05$) as compared to that in the naive control rats (B1). Similarly, the density of α-MSH-ir fibers in the CeA was not altered in conditioned OVX saline treated rats (B4; $p > 0.05$) or nicotine treated intact and OVX rats (B5 and B6; $p > 0.05$) as compared to respective controls. The data are summarized in Fig. 7 F.

DISCUSSION

ICSS reward in OVX rats

In the present study, rats were implanted with the electrode targeted at MFB and trained in the operant chamber for self-stimulation. The consistent lever pressings for 3 consecutive days confirmed that the animals were trained. The use of ICSS to study reward and reinforcement behavior is well established (Carlezon and Chartoff, 2007, Sagara et al., 2008). While the leftward shift in the frequency response curve (FRC) and lowering of ICSS thresholds indicated facilitation of brain stimulation reward, rightward shift of FRC and elevation of thresholds suggested anhedonia (Carlezon and Chartoff, 2007, Vlachou and Markou, 2011; Desai et al., 2013; Somalwar et al., 2017). Herein, the OVX rats showed higher reward threshold and shifted the FRC towards right indicating decreased reward which might be attributed to depleted estrogen. OVX rats showed diminished dopamine in the VTA and reward behavior (Russo et al., 2003). Flores et al. (2016) reported that, estradiol plays an important role in altering dopamine activity in female rats. Estrogen acts on its receptors located on the inhibitory GABAergic terminals in the VTA dopaminergic cell body and inhibits GABAergic transmission which inhibits dopamine release in Acb (Torres et al., 2009). Estrogen is also reported to target presynaptic dopamine terminals and downregulate D2 autoreceptors which eventually increase dopamine release (Becker, 1999). Galankin et al. (2010) demonstrated that estradiol adds to the sensitivity of the brain reward system in rats, which in turn enhances the cocaine effects on the ICSS reward. In this background, we suggest that similar mechanisms may be responsible for the decreased ICSS reward observed in the OVX animals in the present study.

Nicotine-induced brain reward function in OVX rats

Nicotine treatment in OVX rats decreased the threshold and produced reward. The observations are in accordance with the previous report which suggests decreased nicotine reward following ovariectomy in rats (Torres et al., 2009). Nicotine-induced increase in striatal dopamine levels is enhanced via estrogen (Dluzen and Anderson, 1997). Flores and colleagues (2016) also suggested that estradiol enhanced the nicotine induced reward in female rats. Estrogen facilitates dopamine release in the terminal region of the Acb and mediates the rewarding effects of drugs of abuse like nicotine (Becker, 1999). Nicotine amplifies reward signals in the brain, an effect shared by other drugs of abuse (Rice and Cragg, 2004). Consistent with an excitatory action of nicotine on reward circuitries, intravenously self-administered and experimenter administered bolus nicotine injections lowered ICSS thresholds in rats (Huston-Lyons and Kornetsky, 1992; Bauco and Wise, 1994; Harrison et al., 2002; Kenny and Markou, 2006), reflecting nicotine-induced increase in BSR. Nicotine, via nAChRs in the VTA and Acb, activates mesolimbic reward pathway and releases dopamine in the Acb which results in reward behavior (Dani and Heinemann, 1996; Mansvelder and McGehee, 2000; Laviolette and Van der Kooy, 2004). Lesions in the mesolimbic pathway disrupt the self-administration of drugs of abuse (Corrigall et al., 1992; Rassnick et al., 1993; Gerrits and Van Ree, 1996). nAChRs are expressed by excitatory and inhibitory neurons that control excitability of dopamine neurons (Mansvelder et al., 2007). However, single exposure to nicotine increases dopamine release in the Acb for over an hour *in vivo* (Imperato et al., 1986; Schilstrom et al., 1998). Thus, urge of obtaining reward effects may motivate nicotine consumption and contribute to the addictive properties of this drug (Donny et al., 2003; Kenny, 2007).

MCs on reward and reinforcement behavior in OVX rats using ICSS

α-MSH and NDP-MSH, in dose dependent manner, increased the number of lever pressings in OVX rats and shifted the FRC towards left. The leftward shift of FRC suggests reward and reinforcement actions of MCs in the ICSS. Conversely, HS014 decreased the rate of lever pressings which suggests decreased reward. The observation confirms the role of MC4-R in reward and reinforcement action in OVX rats. These results are in accordance with the previous reports. MC agonist infusion into

lateral ventricle or VTA enhanced the dopamine release in the striatum and Acb (Florijn et al., 1993; Lindblom et al., 2001), and administration directly into Acb augmented dopaminergic activity resulting in more grooming (Florijn et al., 1993). Furthermore, *in vitro* studies reveal that α-MSH stimulates cAMP production via interactions with dopamine D1 receptors (Lezcano et al., 1995; Cremer et al., 2000). MC agonist infusion into the lateral ventricle also improved amphetamine reward effect on lateral hypothalamic self-stimulation (Cabeza de Vaca et al., 2002). Hsu et al. (2005) reported that inhibition of MC transmission blocked the cocaine reward. Agonists directly acting on dopamine, or an indirect agonist like cocaine, enhanced POMC expression in the ARC and α-MSH levels in Acb by assisting activation of dopamine neurotransmission (Sarnyai et al., 1992; Tong and Pelletier, 1992). These studies indicate that MC may promote dopaminergic neurotransmission; vice-versa interaction is also suggested.

Expression of MC4-R mRNA in Acb was increased following repeated administration of cocaine (Hsu et al., 2005). Increased MC-4 mRNA expression was also reported in the hypothalamus and amygdala of rats exposed to ethanol (Kokare et al., 2017). In the present study, ICSS conditioned rats showed an increase in MC4-R gene expression in Acb on the ipsilateral side, but a decrease was noted on the contralateral side. While we do not know the underlying reason, we speculate that the decrease may be due to compensatory reduction following ipsilateral increase in MC4-R mRNA. Additional studies will be required to clarify the issue.

Modulation of nicotine-induced reward via MC4-R in ICSS

Several studies have reported a close interaction between nicotinic and MC systems. Altered α-MSH level was found in rat plasma following peripheral administration of nicotine (Conte-Devolx et al., 1981). Hypothalamic α3β4 nAChRs stimulation activated POMC gene and consequently MC4-R expression which is essential for nicotine-induced hypophagia in mice (Mineur et al., 2011). Bellinger and colleagues (2003) reported that icv administration of MTII (melanocortin agonist) reversed nicotine withdrawal induced hyperphagia. On the other hand, continual nicotine exposure inhibited POMC expression and biosynthesis of β-endorphin (endogenous opioid peptide derived from POMC) (Rasmussen, 1998), thus implicating β-endorphin in nicotine self-administration and withdrawal syndrome. More recently, Qi

et al. (2015) suggested a dichotomy in the role of MC4-R in the dysphoria associated with nicotine withdrawal and stress-induced reinstatement of nicotine seeking. Hence, these reports support close association between MC and cholinergic system. Furthermore, in the present study, this association was confirmed in ICSS assay conducted in rats receiving treatment with nicotine and melanocortin. Herein, sub-effective doses of MC agents co-administered with nicotine significantly raised the rate of lever pressings as compared to nicotine *per se.* Similar results were obtained with NDP-MSH administration. On the contrary, HS014 treatment prior to nicotine, attenuated nicotine reward in OVX rats. These results underscore the role of MC4-R in nicotine-induced reward function in OVX rats. Thus, based on these observation we may infer that activation of MC system while attempting the nicotine withdrawal during the menopausal phase may help in easy quitting and without any harmful adverse effects of nicotine.

Effect of ICSS and nicotine treatment on α-MSH-immunoreactivity

To explore the involvement of endogenous MCs in the reward and reinforcement activity of nicotine in OVX rats, we investigated the α-MSH-ir profile in different regions. α-MSH-immunoreactivity in the AcbSh, ARC, BNSTl and PVN was increased in the animals conditioned to self-stimulation. On the other hand, unconditioned or conditioned, OVX animals showed a decrease in the α-MSH-ir density in these regions. A decrease in reward behavior following OVX in rats has been reported (Galankin et al., 2010). Estrogen regulates the POMC gene expression and peptide release (Matsumura et al., 2004). It seems that the depletion of the estrogen levels following OVX might be responsible for the decrease in the MCs in the brain regions. This eventually might decrease the dopamine release in AcbSh and thus influence reward (Fig. 8). In contrast to the results that were obtained in the OVX rats, nicotine treatment increased the α-MSH-ir density in all the aforementioned nuclei. The results are in agreement with the studies showing increased POMC gene expression following nicotine treatment (Mineur et al., 2011). Peripheral nicotine treatment is known to stimulate α-MSH secretion from hypothalamus (Marty et al., 1985; Garnier et al., 1994). Moreover, hypothalamic α3β4 nAChRs stimulation activates POMC gene and consequently MC4-R expression which may be considered as essential component for

nicotine-induced hypophagia in mice (Mineur et al., 2011). Bellinger et al. (2003) reported reversal of nicotine withdrawal symptoms like hyperphagia following treatment with α-MSH agonist. We may recall that co-administration of sub-effective doses of MC agonists and nicotine potentiated the number of lever pressings, suggesting a role for endogenous MCs in nicotine mediated reward. AcbSh, the site for mediating reward behavior, serves as a recipient area for the dopaminergic neurons from VTA (Kleijn et al., 2011) and MC inputs from the ARC (Lutter and Nestler, 2009). Receptors for dopamine as well as MCs are present in the AcbSh (Pandit et al., 2015). In the present study, the increase in the α-MSH fiber density in the AcbSh might be attributed to the increased α-MSH positive cell bodies in the ARC in the nicotine treated conditioned rats. Thus, we propose that the α-MSH may positively modulate the dopamine release and promote reward under the influence of nicotine.

The issues associated with smoking by post-menopausal women, like difficulty in quitting, cannot be over-emphasized. The reward producing action of estradiol may involve cholinergic-melanocortin system which in turn serves as the target for nicotine consumed by the post-menopausal women. We suggest that strategies aimed at testing the intervention with MC4-R may help to address the condition.

Declaration of interest

None

Author's Contribution

MAU, HMU and DMK were responsible for the study concept and design. MAU and HMU contributed to the acquisition of animal data. MAU, HMU and US performed the immunohistochemistry and neuronal tracing studies. MAU, AGC and PC generated cohort and performed qRT-PCR studies. HMU, CDB and MAU assisted with data analysis and NKS, AS, PS and DMK helped in interpretation of findings. HMU, MAU and NKS drafted the manuscript. NKS, AS, PS and DMK provided critical revision of the manuscript for important intellectual content. All authors critically reviewed content and approved final version for publication.

Acknowledgements

Supported by the grants from the University Grants Commission (UGC; F.4-5/151-FRP/2014/BSR), Department of Science and Technology (SR/SO/AS/40/2007), and Department of Biotechnology (BT/PR/14022/Med/30/324/2010), Government of India (GOI), New Delhi, India. This work was also supported by University Research Grant Scheme, Savitribai Phule Pune University and Department Research and Development Program (DRDP) of the Department of Biotechnology, Savitribai Phule Pune University, Pune, India. CDB acknowledges the CSIR for providing senior research fellowship (File no.09/128/0091/2016 EMR-I). PC thanks UGC-GOI for the award of junior research fellowship (UGC-JRF).

References

Ahmed SH, Lutjens R, van der Stap LD, Lekic D, Romano-Spica V, Morales M, et al., 2005. Gene expression evidence for remodeling of lateral hypothalamic circuitry in cocaine addiction. Proc. Nat. Acad. Sci. 102, 11533-11538.

Bauco, P., Wise, R.A., 1994. Potentiation of lateral hypothalamic and midline mesencephalic brain stimulation reinforcement by nicotine: examination of repeated treatment. J. Pharmacol. Exp. Ther. 271, 294-301. PMID: 7965727.

Becker, J.B., 1999. Gender differences in dopaminergic function in striatum and nucleus accumbens. Pharmacol. Biochem. Behav. 64, 803-812. https://doi.org/10.1016/S0091-3057(99)00168-9.

Bellinger, L., Cepeda-Benito, A., Bullard, R.L., Wellman, P.J., 2003. Effect of i.c.v. infusion of the alpha-MSH agonist MTII on meal patterns in male rats following nicotine withdrawal. Life Sci. 73, 1861-1872. https://doi.org/10.1016/S0024-3205(03)00485-5.

Cabeza de Vaca, S., Kim, G.Y., Carr, K.D., 2002. The melanocortin receptor agonist MTII augments the rewarding effect of amphetamine in ad-libitum-fed and food-restricted rats. Psychopharmacology. 161, 77-85. https://doi.org/10.1007/s00213-002-0998-1.

Carlezon, W.A. Jr., Chartoff, E.H., 2007. Intracranial self-stimulation (ICSS) in rodents to study the neurobiology of motivation. Nat. Protoc. 2, 2987-2995. https://doi.org/10.1038/nprot.2007.441.

Conte-Devolx, B., Oliver, C., Giraud, P., Gillioz, P., Castanas, E., Lissitzky, J.C., Boudouresque, F., Millet, Y., 1981. Effect of nicotine on in vivo secretion of

melanocorticotropic hormones in the rat. Life Sci. 28, 1067-1073. https://doi.org/10.1016/0024-3205(81)90755-4.

Corrigall, W.A., Franklin, K.B., Coen, K.M., Clarke, P.B., 1992. The mesolimbic dopaminergic system is implicated in the reinforcing effects of nicotine. Psychopharmacology 107, 285-289. https://doi.org/10.1007/BF02245149.

Coulombe, D., Miliaressis, E., 1987. Fitting intracranial self-stimulation data with growth models. Behav. Neurosci. 101, 209. http://dx.doi.org/10.1037/0735-7044.101.2.209.

Cremer, M.C., de Barioglio, S.R., Celis, M.E., 2000. Interaction between alpha-MSH and acetylcholinergic system upon striatal cAMP and IP_3 levels. Peptides. 21, 699-704. https://doi.org/10.1016/S0196-9781(00)00192-3.

Dani, J.A., Heinemann, S., 1996. Molecular and cellular aspects of nicotine abuse. Neuron. 16, 905-908. https://doi.org/10.1016/S0896-6273(00)80112-9.

Desai, S.J., Bharne, A.P., Upadhya, M.A., Somalwar, A.R., Subhedar, N.K., Kokare, D.M., 2014. A simple and economical method of electrode fabrication for brain self-stimulation in rats. J. Pharmacol. Toxicol. Methods. 69, 141-149. https://doi.org/10.1016/j.vascn.2013.12.006.

Desai, S.J., Upadhya, M.A., Subhedar, N.K., Kokare, D.M., 2013. NPY mediates reward activity of morphine, via NPY Y1 receptors, in the nucleus accumbens shell. Behav. Brain. Res. 247, 79-91. https://doi.org/10.1016/j.bbr.2013.03.018.

Dluzen, D.E., Anderson, L.I., 1997. Estrogen differentially modulates nicotine-evoked dopamine release from the striatum of male and female rats. Neurosci. Lett. 230, 140-142. https://doi.org/10.1016/S0304-3940(97)00487-4.

Donny, E.C., Chaudhri, N., Caggiula, A.R., Evans-Martin, F.F., Booth, S., Gharib, M.A., et al., 2003. Operant responding for a visual reinforcer in rats is enhanced by noncontingent nicotine: implications for nicotine self-administration and reinforcement. Psychopharmacology. 169, 68-76. https://doi.org/10.1007/s00213-003-1473-3.

Elias, C.F., Lee, C., Kelly, J., Aschkenasi, C., Ahima, R.S., Couceyro, P.R., Kuhar, M.J., Saper, C.B., Elmquist, J.K., 1998a. Leptin activates hypothalamic CART neurons projecting to the spinal cord. Neuron. 21, 1375-1385. https://doi.org/10.1016/S0896-6273(00)80656-X.

Elias, C.F., Saper, C.B., Maratos-Flier, E., Tritos, N.A., Lee, C., Kelly, J., Tatro, J.B., Hoffman, G.E., Ollmann, M.M., Barsh, G.S., Sakurai, T., 1998b. Chemically defined projections linking the mediobasal hypothalamus and the lateral hypothalamic area. J Comp. Neurol. 402, 442-459. https://doi.org/10.1002/(SICI)1096-9861(19981228)402:4%3C442::AID-CNE2%3E3.0.CO;2-R.

Fekete, C., Légrádi, G., Mihály, E., Tatro, J.B., Rand, W.M., Lechan, R.M., 2000. Alpha-Melanocyte stimulating hormone prevents fasting-induced suppression of corticotropin-releasing hormone gene expression in the rat hypothalamic paraventricular nucleus. Neurosci. Lett. 289, 152-156. https://doi.org/10.1016/S0304-3940(00)01256-8.

Flores, R.J., Pipkin, J.A., Uribe, K.P., Perez, A., O'Dell, L.E., 2016. Estradiol promotes the rewarding effects of nicotine in female rats. Behav. Brain. Res. 307, 258-263. https://doi.org/10.1016/j.bbr.2016.04.004.

Florijn, W.J., Holtmaat, A.J., de Lang, H., Spierenburg, H., Gispen, W.H., Versteeg, D.H., 1993. Peptide-induced grooming behavior and caudate nucleus dopamine release. Brain. Res. 625, 169-172. https://doi.org/10.1016/0006-8993(93)90151-c.

Galankin, T., Shekunova, E., Zvartau, E., 2010. Estradiol lowers intracranial self-stimulation thresholds and enhances cocaine facilitation of intracranial self-stimulation in rats. Horm. Behav. 58, 827-834. https://doi.org/10.1016/j.yhbeh.2010.08.006.

Garnier, M., Lamacz, M., Tonon, M.C., Vaudry, H., 1994. Functional characterization of a nonclassical nicotine receptor associated with inositolphospholipid breakdown and mobilization of intracellular calcium pools. Proc. Natl. Acad. Sci. USA. 91, 11743-11747. https://doi.org/10.1073/pnas.91.24.11743.

Gerrits, M.A., Van Ree, J.M., 1996. Effect of nucleus accumbens dopamine depletion on motivational aspects involved in initiation of cocaine and heroin self-administration in rats. Brain. Res. 713, 114-124. https://doi.org/10.1016/0006-8993(95)01491-8.

Harrison, A.A., Gasparini, F., Markou, A., 2002. Nicotine potentiation of brain stimulation reward reversed by DH beta E and SCH 23390, but not by eticlopride, LY 314582 or MPEP in rats. Psychopharmacology. 160, 56-66. https://doi.org/10.1007/s00213-001-0953-6

Hsu, R., Taylor, J.R., Newton, S.S., Alvaro, J.D., Haile, C., Han, G., Hruby, V.J., Nestler, E.J., Duman, R.S., 2005. Blockade of melanocortin transmission inhibits cocaine reward. Eur. J. Neurosci. 21, 2233-2242. https://doi.org/10.1111/j.1460-9568.2005.04038.x.

Huston-Lyons, D., Kornetsky, C., 1992. Effects of nicotine on the threshold for rewarding brain stimulation in rats. Pharmacol. Biochem. Behav. 41, 755-759. https://doi.org/10.1016/0091-3057(92)90223-3.

Imperato, A., Mulas, A., Di Chiara, G., 1986. Nicotine preferentially stimulates dopamine release in the limbic system of freely moving rats. Eur. J. Pharmacol. 132, 337-338. https://doi.org/10.1016/0014-2999(86)90629-1.

Jaimes, E.A., Tian, R.X., Joshi, M.S., Raij, L., 2009. Nicotine augments glomerular injury in a rat model of acute nephritis. Am. J. Nephrol. 29, 319-326. https://doi.org/10.1159/000163593.

Kenny, P.J., Markou, A., 2006. Nicotine self-administration acutely activates brain reward systems and induces a long-lasting increase in reward sensitivity. Neuropsychopharmacology. 31, 1203-1211. https://doi.org/10.1038/sj.npp.1300905.

Kenny, P.J., 2007. Brain reward systems and compulsive drug use. Trends. Pharmacol. Sci. 28, 135-141. https://doi.org/10.1016/j.tips.2007.01.008.

Kleijn, J., Folgering, J.H., van der Hart, M.C., Rollema, H., Cremers, T.I., Westerink, B.H., 2011. Direct effect of nicotine on mesolimbic dopamine release in rat nucleus accumbens shell. Neurosci. Lett. 493, 55-58. https://doi.org/10.1016/j.neulet.2011.02.035.

Kokare, D.M., Dandekar, M.P., Singru, P.S., Gupta, G.L., Subhedar, N.K., 2010. Involvement of alpha-MSH in the social isolation induced anxiety- and depression-like behaviors in rat. Neuropharmacology 58, 1009-1018. https://doi.org/10.1016/j.neuropharm.2010.01.006.

Kokare, D.M., Kyzar, E.J., Zhang, H., Sakharkar, A.J., Pandey, S.C., 2017. Adolescent alcohol exposure-induced changes in alpha-melanocyte stimulating hormone and neuropeptide y pathways via histone acetylation in the brain during adulthood. Int. J. Neuropsychopharmacol. 20, 758-768. https://doi.org/10.1093/ijnp/pyx041.

Kokare, D.M., Shelkar, G.P., Borkar, C.D., Nakhate, K.T., Subhedar, N.K., 2011. A simple and inexpensive method to fabricate a cannula system for intracranial injections in rats and mice. J. Pharmacol. Toxicol. Methods. 64, 246-250. https://doi.org/10.1016/j.vascn.2011.08.002.

Koob G, 2000. Drug addiction. Neurobiol. Dis. 7, 543-545.

Laviolette, S.R., van der Kooy, D., 2004. The neurobiology of nicotine addiction: bridging the gap from molecules to behaviour. Nat. Rev. Neurosci. 5, 55-65. https://doi.org/10.1038/nrn1298.

Lee, J., Cooke, J.P., 2011. The role of nicotine in the pathogenesis of atherosclerosis. Atherosclerosis. 215, 281-283. https://doi.org/10.1016/j.atherosclerosis.2011.01.003.

Lezcano, N.E., De Barioglio, S.R., Celis, M.E., 1995. Alpha-MSH changes cyclic AMP levels in rat brain slices by an interaction with the D1 dopamine receptor. Peptides. 16, 133-137. https://doi.org/10.1016/0196-9781(94)00157-2.

Lindblom, J., Opmane, B., Mutulis, F., Mutule, I., Petrovska, R., Klusa, V., Bergström, L., Wikberg, J.E., 2001. The MC4 receptor mediates alpha-MSH induced release of nucleus accumbens dopamine. NeuroReport. 12, 2155-2158. https://doi.org/10.1097/00001756-200107200-00022.

Livak, K.J., Schmittgen, T.D., 2001. Analysis of relative gene expression data using real-time quantitative PCR and the 2− ΔΔCT method. Methods, 25, 402-408. https://doi.org/10.1006/meth.2001.1262.

Lutter, M., Nestler, E.J., 2009. Homeostatic and hedonic signals interact in the regulation of food intake. J. Nutr. 139, 629-632. https://doi.org/10.3945/jn.108.097618.

Mansvelder, H.D., Fagen, Z.M., Chang, B., Mitchum, R., McGehee, D.S., 2007. Bupropion inhibits the cellular effects of nicotine in the ventral tegmental area. Biochem. Pharmacol. 74, 1283-1291. https://doi.org/10.1016/j.bcp.2007.07.034.

Mansvelder, H.D., McGehee, D.S., 2000. Long-term potentiation of excitatory inputs to brain reward areas by nicotine. Neuron. 27, 349-357. https://doi.org/10.1016/S0896-6273(00)00042-8.

Marty, M.A., Erwin, V.G., Cornell, K., Zgombick, J.M., 1985. Effects of nicotine on beta-endorphin, alpha MSH, and ACTH secretion by isolated perfused mouse brains and pituitary glands, in vitro. Pharmacol. Biochem. Behav. 22, 317-325. https://doi.org/10.1016/0091-3057(85)90397-1.

Matsumura, R., Takeuchi, S., Takahashi, S., 2004. Effect of estrogen on melanocortin-3 receptor mRNA expression in mouse pituitary glands in vivo and in vitro. Neuroendocrinology. 80, 143-151. https://doi.org/10.1159/000082355.

Mineur, Y.S., Abizaid, A., Rao, Y., Salas, R., DiLeone, R.J., Gündisch, D., et al., 2011. Nicotine decreases food intake through activation of POMC neurons. Science. 332, 1330-1332. https://doi.org/10.1126/science.1201889.

Miliaressis, E., Rompré, P.P., Durivage, A., 1982. Psychophysical method for mapping behavioral substrates using a moveable electrode. Brain. Res. Bull. 8, 693-701. https://doi.org/10.1016/0361-9230(82)90097-1.

Pandit, R., Van Der Zwaal, E.M., Luijendijk, M.C., Brans, M.A., Van Rozen, A.J., Ophuis, R.J., et al., 2015. Central melanocortins regulate the motivation for sucrose reward. PLoS. One. 10, e0121768. https://doi.org/10.1371/journal.pone.0121768.

Paxinos, G., Watson, C., 1998. The rat brain in stereotaxic coordinates. Academic. Press. London.

Peltier, M.R., Flores, J.M., Smith, P.H., Roberts, W., Verplaetse, T.L., Moore, K.E., 2019. Smoking across the menopausal transition in a 10-year longitudinal sample: The role of sex hormones and depressive symptoms. Nicotine Tob. Res. pii: ntz069. https://doi: 10.1093/ntr/ntz069.

Qi, X., Yamada, H., Corrie, L.W., Ji, Y., Bauzo, R.M., Alexander, J.C., Bruijnzeel, A.W., 2015. A critical role for the melanocortin 4 receptor in stress-induced relapse to nicotine seeking in rats. Addict. Biol. 20, 324-335. https://doi.org/10.1111/adb.12129.

Rasmussen, D.D., 1998. Effects of chronic nicotine treatment and withdrawal on hypothalamic proopiomelanocortin gene expression and neuroendocrine regulation. Psychoneuroendocrinology. 23, 245-259. https://doi.org/10.1016/S0306-4530(98)00003-1.

Rassnick, S., Stinus, L., Koob, G.F., 1993. The effects of 6-hydroxydopamine lesions of the nucleus accumbens and the mesolimbic dopamine system on oral self-administration of ethanol in the rat. Brain. Res. 623, 16-24. https://doi.org/10.1016/0006-8993(93)90004-7.

Rice, M.E., Cragg, S.J., 2004. Nicotine amplifies reward-related dopamine signals in striatum. Nat. Neurosci. 7, 583-584. https://doi.org/10.1038/nn1244.

Russo, S.J., Festa, E.D., Fabian, S.J., Gazi, F.M., Kraish, M., Jenab, S., Quiñones-Jenab, V., 2003. Gonadal hormones differentially modulate cocaine-induced conditioned place preference in male and female rats. Neuroscience. 120, 523-533. https://doi.org/10.1016/S0306-4522(03)00317-8.

Sagara, H., Kitamura, Y., Yae, T., Shibata, K., Suemaru, K., Sendo, T., et al., 2008. Nicotinic acetylcholine alpha4beta2 receptor regulates the motivational effect of

intracranial self stimulation behavior in the runway method. J. Pharmacol. Sci. 108, 455-461. https://doi.org/10.1254/jphs.08168FP.

Sagarkar, S., Bhamburkar, T., Shelkar, G., Choudhary, A., Kokare, D.M., Sakharkar, A.J., 2017. Minimal traumatic brain injury causes persistent changes in DNA methylation at BDNF gene promoters in rat amygdala: a possible role in anxiety-like behaviors. Neurobiol. Dis. 106, 101-109. https://doi.org/10.1016/j.nbd.2017.06.016.

Sarnyai, Z., Vecsernyés, M., Julesz, J., Szabó, G., Telegdy, G., 1992. Effects of cocaine and pimozide on plasma and brain alpha-melanocyte-stimulating hormone levels in rats. Neuroendocrinology. 55, 9-13. https://doi.org/10.1159/000126090.

Schilstrom, B., Nomikos, G.G., Nisell, M., Hertel, P., Svensson, T.H., 1998. *N*-Methyl-D-aspartate receptor antagonism in the ventral tegmental area diminishes the systemic nicotine-induced dopamine release in the nucleus accumbens. Neuroscience. 82, 781-789. https://doi.org/10.1016/S0306-4522(97)00243-1.

Shelkar, G.P., Kale, A.D., Singh, U., Singru, P.S., Subhedar, N.K., Kokare, D.M., 2015. Alpha-melanocyte stimulating hormone modulates ethanol self-administration in posterior ventral tegmental area through melanocortin-4 receptors. Addict. Biol. 20, 302-315. https://doi.org/10.1111/adb.12126.

Singru, P.S., Fekete, C., Lechan, R.M., 2005. Neuroanatomical evidence for participation of the hypothalamic dorsomedial nucleus (DMN) in regulation of the hypothalamic paraventricular nucleus (PVN) by alpha-melanocyte stimulating hormone. Brain Res. 1064, 42-51. https://doi.org/10.1016/j.brainres.2005.09.023.

Somalwar, A.R., Shelkar, G.P., Subhedar, N.K., Kokare, D.M., 2017. The role of neuropeptide CART in the lateral hypothalamic-ventral tegmental area (LH-VTA) circuit in motivation. Behav. Brain. Res. 317, 340-349. https://doi.org/10.1016/j.bbr.2016.09.054.

Tapinc, D.E., Ilgin, R., Kaya, E., Gozen, O., Ugur, M., Koylu, E.O., et al., 2017. Gene expression of pro-opiomelanocortin and melanocortin receptors is regulated in the hypothalamus and mesocorticolimbic system following nicotine administration. Neurosci. Lett. 637, 75-79. https://doi.org/10.1016/j.neulet.2016.11.049.

Tong, Y., Pelletier, G., 1992. Role of dopamine in the regulation of proopiomelanocortin (POMC) mRNA levels in the arcuate nucleus and pituitary gland of the female rat as studied by in situ hybridization. Brain. Res. 15, 27-32. https://doi.org/10.1016/0169-328X(92)90147-4.

Torres, O.V., Natividad, L.A., Tejeda, H.A., Van Weelden, S.A., O'Dell, L.E., 2009. Female rats display dose-dependent differences to the rewarding and aversive effects of nicotine in an age-, hormone-, and sex-dependent manner. Psychopharmacology. 206, 303-312. https://doi.org/10.1007/s00213-009-1607-3.

Upadhya, M.A., Nakhate, K.T., Kokare, D.M., Singh, U., Singru, P.S., Subhedar, N.K., 2012. CART peptide in the nucleus accumbens shell acts downstream to dopamine and mediates the reward and reinforcement actions of morphine.

Neuropharmacology. 62, 1823-1833. https://doi.org/10.1016/j.neuropharm.2011.12.004.

Vlachou, S., Markou, A., 2011. Intracranial Self-Stimulation. In: Mary C. Olmstead, (ed). Animal Models of Drug Addiction. Neuromethods. 53, 3-56. https://doi.org/10.1007/978-1-60761-934-5_1.

Wassenaar, C.A., Dong, Q., Amos, C.I., Spitz, M.R., Tyndale, R.F., 2013. Pilot study of CYP2B6 genetic variation to explore the contribution of nitrosamine activation to lung carcinogenesis. Int. J. Mol. Sci. 14, 8381-8392. http://dx.doi.org/10.3390/ijms14048381.

Wise, R.A., 1996. Addictive drugs and brain stimulation reward. Annu. Rev. Neurosci. 19, 319-340. https://doi.org/10.1146/annurev.ne.19.030196.001535.

FIGURE LEGENDS:

Fig. 1. Schematic drawing of the coronal section (A) through the brain of rat [−2.8 mm posterior to the bregma (Paxinos and Watson, 1998)] showing the position of the electrode tip (black circle) in the lateral hypothalamus-medial forebrain (LH-MFB) and passage of electrode (B; asterisks) directed toward the LH-MFB (Scale bar = 500 µm). C represents the schematic diagram at the level of Acb from where the tissue was isolated for MC4-R mRNA expression. The effect of intracranial self-stimulation (ICSS), on melanocortin-4 receptors (MC4-R) mRNA expression in the nucleus accumbens (Acb) is shown in D. The graphs represent the means ± SEM values for fold changes in the MC4-R mRNA expression across ipsilateral and contralateral Acb regions in the control and ICSS groups (n = 4 rats/group). The data were analyzed by non-parametric t-test. *$p < 0.05$ vs ipsilateral control, $^{\#}p < 0.05$ vs contralateral control. Figure E represents the staining specificity for α-MSH-immunoreactivity at the level of arcuate nucleus of hypothalamus (ARC) in the presence of α-MSH antibody E(i) and its respective preadsorption control E(ii). Scale bar = 50 µm. 3V, third Ventricle.

Fig. 2. Effect of ovariectomy (OVX, n = 6-8 rats/group; A-C), and saline (n = 6 rats/group; ip), nicotine in intact (NIC, n = 5 rats/group; ip; D-F) and OVX (NIC, n = 8 rats/group; ip; G-I) rats on intracranial self-stimulation (ICSS) activity. The data represents the number of lever pressings (A, D and G), M_{50} (B, E and H) and T_0 (C, F and I). Each bar represents the mean ± SEM. The post-hoc Bonferroni's multiple comparison test revealed the significance value for the condition and nicotine treatment *$p < 0.05$, **$p < 0.01$, ***$p < 0.001$ versus respective baseline control and $^{\$}p < 0.05$, $^{\$\$\$}p < 0.001$ versus respective Sham control.

Fig. 3. Effect of artificial cerebrospinal fluid (aCSF, n = 7 rats/group; icv), alpha-melanocyte stimulating hormone (α-MSH, n = 7 rats/group; icv; A-C), NDP-MSH (n = 6 rats/group; icv; D-F), HS014 (n = 6 rats/group; icv; G-I) on intracranial self-stimulation (ICSS) activity of ovariectomized rats. The data represents the number of lever pressings (A, D and G), M_{50} (B, E and H) and T_0 (C, F and I). Each bar represents the mean ± SEM. The post-hoc Bonferroni's multiple comparison test revealed the significance value for the treatments *$p < 0.05$, **$p < 0.01$, ***$p < 0.001$ versus respective control.

Fig. 4. Graph representing the effect of alpha-melanocyte stimulating hormone (α-MSH, n = 6 rats/group; icv; A-C), NDP-MSH (n = 7 rats/group; icv; D-F) and HS014 (n = 6 rats/group; icv; G-I) prior to nicotine (NIC, ip) in ovariectomized rats on intracranial self-

stimulation (ICSS) activity. The data represents the number of lever pressings (A, D, G, H and M), M_{50} (B, E, H, K and N) and T_0 (C, F, I, L and O). Each bar represents the mean ± SEM. The post-hoc Bonferroni's multiple comparison test revealed the significance value for the treatments *p < 0.05, **p < 0.01, ***p < 0.001 versus respective aCSF control and $^{\#}p < 0.05$, $^{\#\#}p < 0.01$, $^{\#\#\#}p < 0.001$ versus respective NIC control.

Fig. 5. Photomicrographs of coronal section showing alpha-melanocyte stimulating hormone (α-MSH) immunoreactive cells (arrow heads) and fibers (arrows) in the nucleus accumbens shell (AcbSh; A1-A6), arcuate nucleus of hypothalamus (ARC; B1-B6) and lateral part of bed nucleus of stria terminalis (BNSTl; C1-C6) of the unconditioned naïve control (A1, B1, C1), ovariectomized rats (OVX; A2, B2, C2), saline treated intact control (intact+saline; A3, B3, C3), saline treated ovarectomized (OVX+saline; A4, B4, C4), nicotine treated intact (intact+nicotine; A5, B5, C5), nicotine treated ovarectomized (OVX+nicotine; A6, B6, C6) operant conditioned rats. Scale bar = 50 µm. 3V, third ventricle; aca, anterior commissure (anterior part).

Fig. 6. Photomicrographs of coronal section showing alpha-melanocyte stimulating hormone (α-MSH) immunoreactive cells (arrow heads) and fibers (arrows) in the paraventricular nucleus of hypothalamus (PVN; A1-A6) and central nucleus of amygdala (CeA; B1-B6) of the unconditioned naïve control (A1 and B1), ovariectomized rats (OVX; A2 and B2), saline treated intact control (intact+saline; A3 and B3), saline treated ovarectomized (OVX+saline; A4 and B4), nicotine treated intact (intact+nicotine; A5 and B5), nicotine treated ovarectomized (OVX+nicotine; A6 and B6) operant conditioned rats. Scale bar = 50 µm. 3V, third ventricle.

Fig. 7. Semiquantitative morphometric analysis of alpha-melanocyte stimulating hormone (α-MSH) immunoreactive (ir) content the nucleus accumbens shell (AcbSh; A), the arcuate nucleus of hypothalamus (ARC; B and C), the lateral part of bed nucleus of stria terminalis (BNSTl; D), the paraventricular nucleus of hypothalamus (PVN; E) and the central nucleus of amygdala (CeA; F) of the unconditioned naïve control, OVX and saline or nicotine treated intact and/or ovariectomized (OVX) operant conditioned rats. The outline of the transverse section through the brain [co-ordinates: bregma +0.7 mm (AcbSh), −2.56 mm (ARC), -0.26 (BNSTl), −1.80 mm (PVN) and −2.56 mm (CeA) (Paxinos and Watson, 1998)] indicates the respective regions (square, not to scale) from which the measurements were collated. The bar values are shown as the mean ± SEM of five measurements from AcbSh, ARC, BNSTl, PVN and CeA on both the sides of each brain (n = 5 rats/group). The data were analyzed by one-way ANOVA followed

by post-hoc Bonferroni's multiple comparison test. **p < 0.01, ***p < 0.001 versus Naïve control; #p<0.05, ##p<0.01, ###p<0.001 versus Intact+Saline conditioned rats and $$$p < 0.001 versus OVX+saline conditioned rats. 3V, third ventricle; ac, anterior commissure; aca, anterior commissure (anterior part); AcbC, nucleus accumbens core; acp, anterior commissure (posterior part); AHC, central part of anterior hypothalamic area; BLA, lateral part of basolateral amygdaloid nucleus; DMH, dorsomedial hypothalamic nucleus; LGP, lateral globus pallidus; LSV, ventral part of lateral septal nucleus; LV, lateral ventricle; MeAD, medial amygdaloid nucleus, anterodorsal part; opt, optic tract; Rch, retrochiasmatic area and VMH, ventromedial hypothalamic nucleus.

Fig. 8. Hypothesized mechanism: Nicotine may act presynaptically on the pro-opiomelanocortins (POMC) containing axonal terminals of arcuate (ARC) neurons, which may be under the influence of peripheral estrogen. α-MSH released by the POMC neurons may modulate the reward behavior via release of dopamine in the frame of the nucleus accumbens (Acb). α-MSH, alpha-melanocyte stimulating hormone; AcbSh, accumbens shell; DA, dopamine; LH-MFB, lateral hypothalamus-medial forebrain bundle; MC4-R, melanocortin-4 receptors; nAchRs, nicotinic cholinergic receptors; OVX, ovariectomized; VTA, ventral tegmentum area. (1) Flores et al., 2016; (2) Lutter and Nestler, 2009; (3) Wise 1996; (4) Mineur et al., 2011; (5) Lindblom et al., 2001.

FIGURE LEGENDS:

Fig. 1. Schematic drawing of the coronal section (A) through the brain of rat [−2.8 mm posterior to the bregma (Paxinos and Watson, 1998)] showing the position of the electrode tip (black circle) in the lateral hypothalamus-medial forebrain (LH-MFB) and passage of electrode (B; asterisks) directed toward the LH-MFB (Scale bar = 500 µm). C represents the schematic diagram at the level of Acb from where the tissue was isolated for MC4-R mRNA expression. The effect of intracranial self-stimulation (ICSS), on melanocortin-4 receptors (MC4-R) mRNA expression in the nucleus accumbens (Acb) is shown in D. The graphs represent the means ± SEM values for fold changes in the MC4-R mRNA expression across ipsilateral and contralateral Acb regions in the control and ICSS groups (n = 4 rats/group). The data were analyzed by non-parametric t-test. *p < 0.05 vs ipsilateral control, #p < 0.05 vs contralateral control. Figure E represents the staining specificity for α-MSH-immunoreactivity at the level of arcuate nucleus of hypothalamus (ARC) in the presence of α-MSH antibody E(i) and its respective preadsorption control E(ii). Scale bar = 50 µm. 3V, third Ventricle.

Fig. 2. Effect of ovariectomy (OVX, n = 6-8 rats/group; A-C), and saline (n = 6 rats/group; ip), nicotine in intact (NIC, n = 5 rats/group; ip; D-F) and OVX (NIC, n = 8

rats/group; ip; G-I) rats on intracranial self-stimulation (ICSS) activity. The data represents the number of lever pressings (A, D and G), M_{50} (B, E and H) and T_0 (C, F and I). Each bar represents the mean ± SEM. The post-hoc Bonferroni's multiple comparison test revealed the significance value for the condition and nicotine treatment *p < 0.05, **p < 0.01, ***p < 0.001 versus respective baseline control and $^{\$}$p < 0.05, $^{\$\$\$}$p < 0.001 versus respective Sham control.

Fig. 3. Effect of artificial cerebrospinal fluid (aCSF, n = 7 rats/group; icv), alpha-melanocyte stimulating hormone (α-MSH, n = 7 rats/group; icv; A-C), NDP-MSH (n = 6 rats/group; icv; D-F), HS014 (n = 6 rats/group; icv; G-I) on intracranial self-stimulation (ICSS) activity of ovariectomized rats. The data represents the number of lever pressings (A, D and G), M_{50} (B, E and H) and T_0 (C, F and I). Each bar represents the mean ± SEM. The post-hoc Bonferroni's multiple comparison test revealed the significance value for the treatments *p < 0.05, **p < 0.01, ***p < 0.001 versus respective control.

Fig. 4. Graph representing the effect of alpha-melanocyte stimulating hormone (α-MSH, n = 6 rats/group; icv; A-C), NDP-MSH (n = 7 rats/group; icv; D-F) and HS014 (n = 6 rats/group; icv; G-I) prior to nicotine (NIC, ip) in ovariectomized rats on intracranial self-stimulation (ICSS) activity. The data represents the number of lever pressings (A, D, G, H and M), M_{50} (B, E, H, K and N) and T_0 (C, F, I, L and O). Each bar represents the mean ± SEM. The post-hoc Bonferroni's multiple comparison test revealed the significance value for the treatments *p < 0.05, **p < 0.01, ***p < 0.001 versus respective aCSF control and $^{\#}$p < 0.05, $^{\#\#}$p < 0.01, $^{\#\#\#}$p < 0.001 versus respective NIC control.

Fig. 5. Photomicrographs of coronal section showing alpha-melanocyte stimulating hormone (α-MSH) immunoreactive cells (arrow heads) and fibers (arrows) in the nucleus accumbens shell (AcbSh; A1-A6), arcuate nucleus of hypothalamus (ARC; B1-B6) and lateral part of bed nucleus of stria terminalis (BNSTl; C1-C6) of the unconditioned naïve control (A1, B1, C1), ovariectomized rats (OVX; A2, B2, C2), saline treated intact control (intact+saline; A3, B3, C3), saline treated ovarectomized (OVX+saline; A4, B4, C4), nicotine treated intact (intact+nicotine; A5, B5, C5), nicotine treated ovarectomized (OVX+nicotine; A6, B6, C6) operant conditioned rats. Scale bar = 50 µm. 3V, third ventricle; aca, anterior commissure (anterior part).

Fig. 6. Photomicrographs of coronal section showing alpha-melanocyte stimulating hormone (α-MSH) immunoreactive cells (arrow heads) and fibers (arrows) in the

paraventricular nucleus of hypothalamus (PVN; A1-A6) and central nucleus of amygdala (CeA; B1-B6) of the unconditioned naïve control (A1 and B1), ovariectomized rats (OVX; A2 and B2), saline treated intact control (intact+saline; A3 and B3), saline treated ovarectomized (OVX+saline; A4 and B4), nicotine treated intact (intact+nicotine; A5 and B5), nicotine treated ovarectomized (OVX+nicotine; A6 and B6) operant conditioned rats. Scale bar = 50 μm. 3V, third ventricle.

Fig. 7.Semiquantitative morphometric analysis of alpha-melanocyte stimulating hormone (α-MSH) immunoreactive (ir) content the nucleus accumbens shell (AcbSh; A), the arcuate nucleus of hypothalamus (ARC; B and C), the lateral part of bed nucleus of stria terminalis (BNSTl; D), the paraventricular nucleus of hypothalamus (PVN; E) and the central nucleus of amygdala (CeA; F) of the unconditioned naïve control, OVX and saline or nicotine treated intact and/or ovariectomized (OVX) operant conditioned rats. The outline of the transverse section through the brain [co-ordinates: bregma +0.7 mm (AcbSh), −2.56 mm (ARC), -0.26 (BNSTl), −1.80 mm (PVN) and −2.56 mm (CeA) (Paxinos and Watson, 1998)] indicates the respective regions (square, not to scale) from which the measurements were collated. The bar values are shown as the mean ± SEM of five measurements from AcbSh, ARC, BNSTl, PVN and CeA on both the sides of each brain (n = 5 rats/group). The data were analyzed by one-way ANOVA followed by post-hoc Bonferroni's multiple comparison test. **p < 0.01, ***p < 0.001 versus Naïve control; $^{\#}$p<0.05, $^{\#\#}$p<0.01, $^{\#\#\#}$p<0.001 versus Intact+Saline conditioned rats and $^{\$\$\$}$p < 0.001 versus OVX+saline conditioned rats. 3V, third ventricle; ac, anterior commissure; aca, anterior commissure (anterior part); AcbC, nucleus accumbens core; acp, anterior commissure (posterior part); AHC, central part of anterior hypothalamic area; BLA, lateral part of basolateral amygdaloid nucleus; DMH, dorsomedial hypothalamic nucleus; LGP, lateral globus pallidus; LSV, ventral part of lateral septal nucleus; LV, lateral ventricle; MeAD, medial amygdaloid nucleus, anterodorsal part; opt, optic tract; Rch, retrochiasmatic area and VMH, ventromedial hypothalamic nucleus.

Fig. 8. Hypothesized mechanism: Nicotine may act presynaptically on the pro-opiomelanocortins (POMC) containing axonal terminals of arcuate (ARC) neurons, which may be under the influence of peripheral estrogen. α-MSH released by the POMC neurons may modulate the reward behavior via release of dopamine in the frame of the nucleus accumbens (Acb). α-MSH, alpha-melanocyte stimulating hormone; AcbSh, accumbens shell; DA, dopamine; LH-MFB, lateral hypothalamus-medial forebrain bundle; MC4-R, melanocortin-4 receptors; nAchRs, nicotinic cholinergic receptors; OVX, ovariectomized; VTA, ventral tegmentum area. (1) Flores et al., 2016; (2) Lutter and Nestler, 2009; (3) Wise 1996; (4) Mineur et al., 2011; (5) Lindblom et al., 2001.

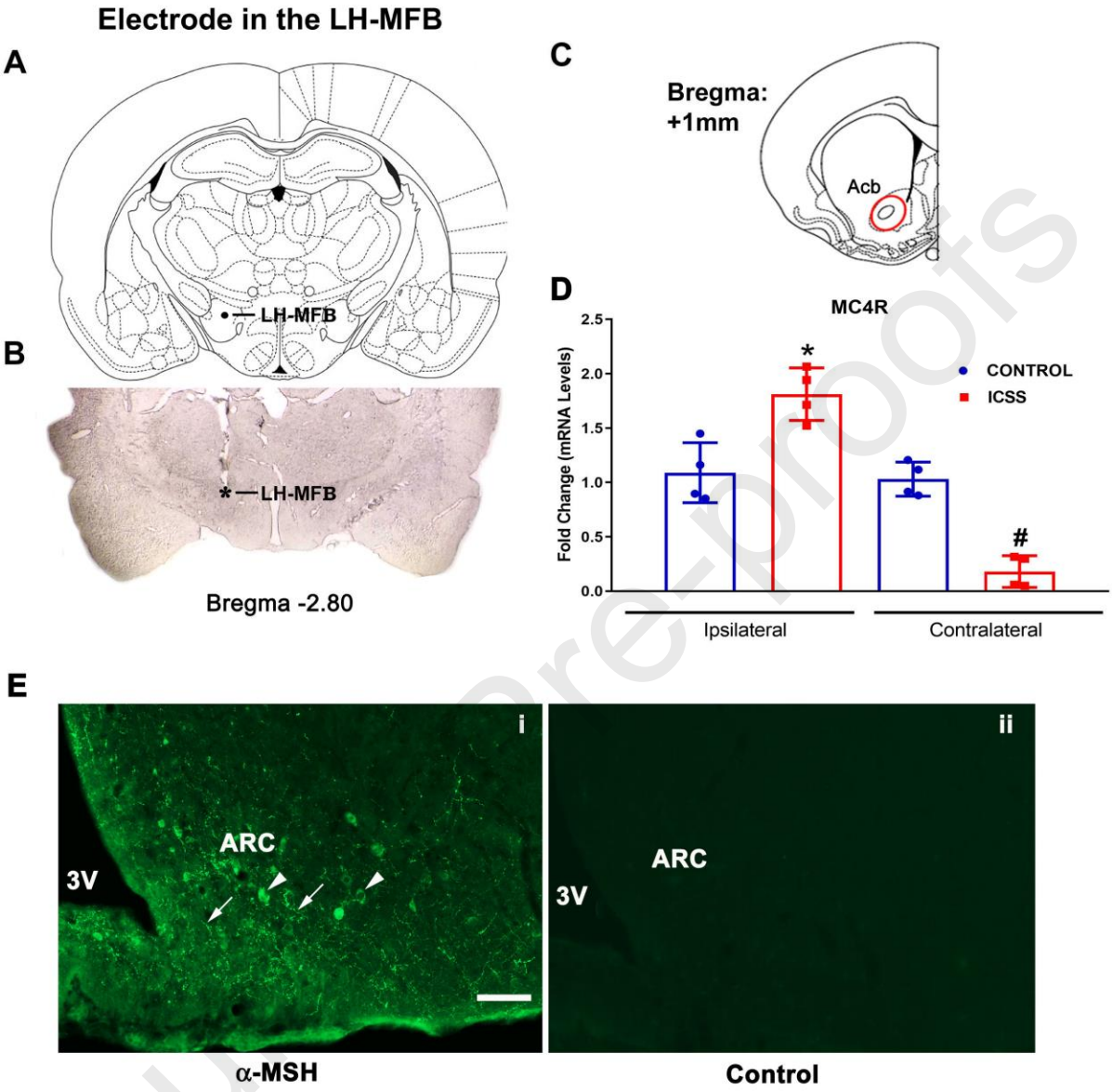

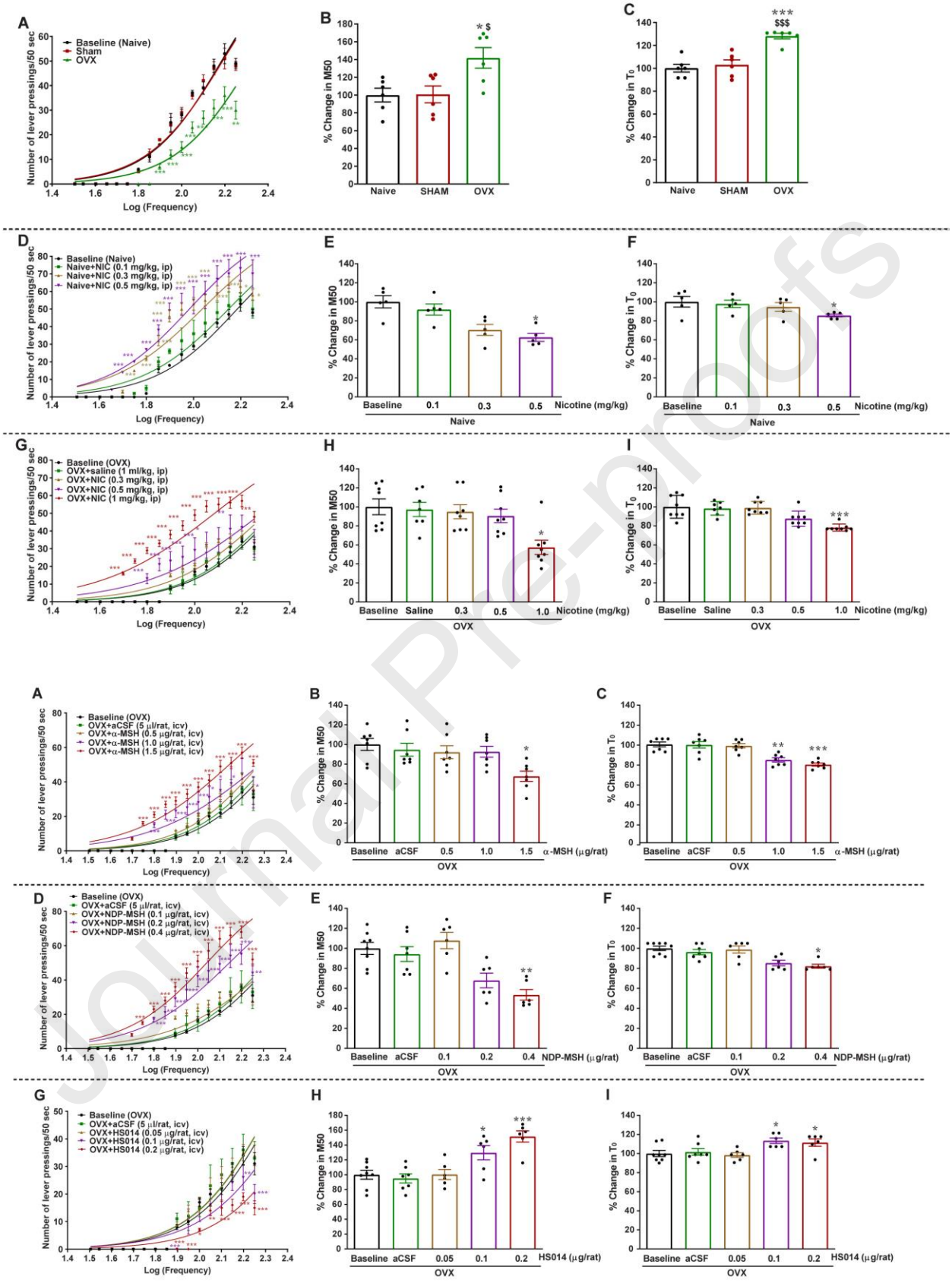

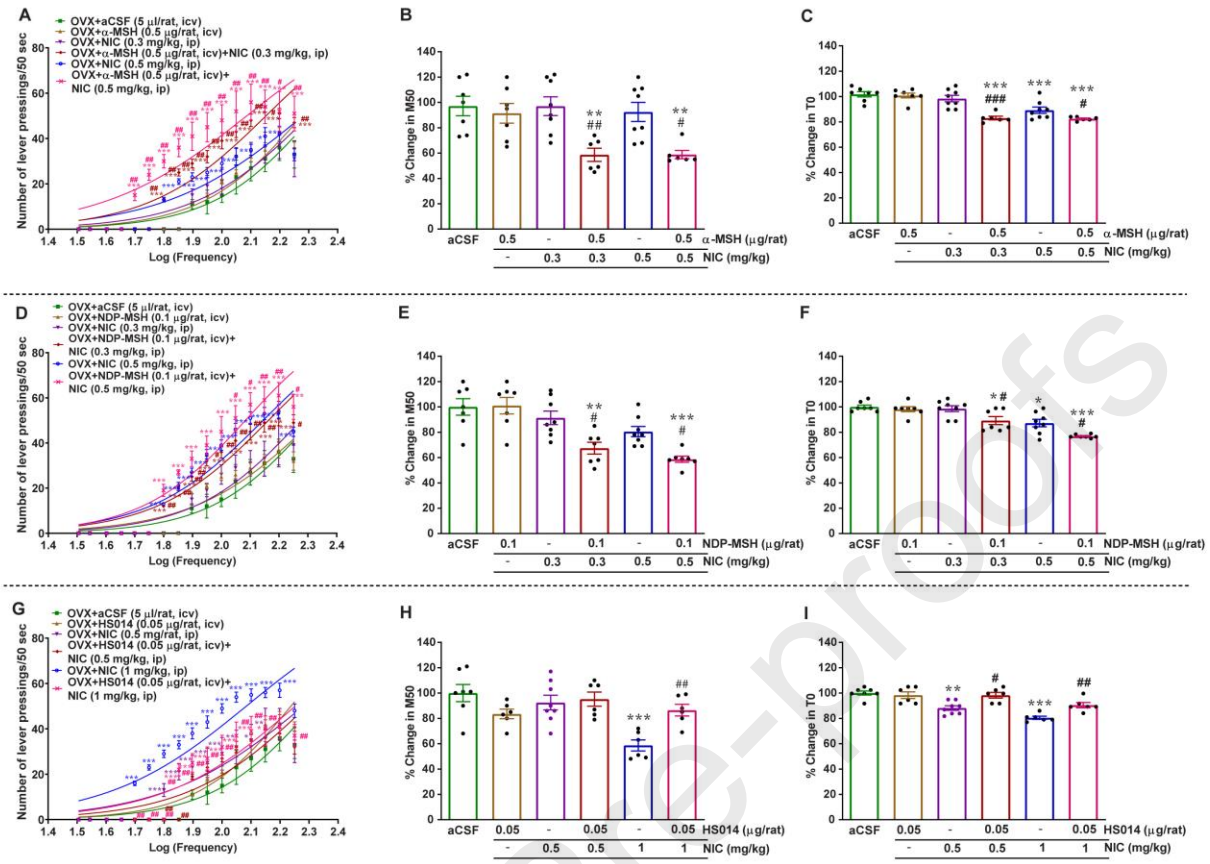

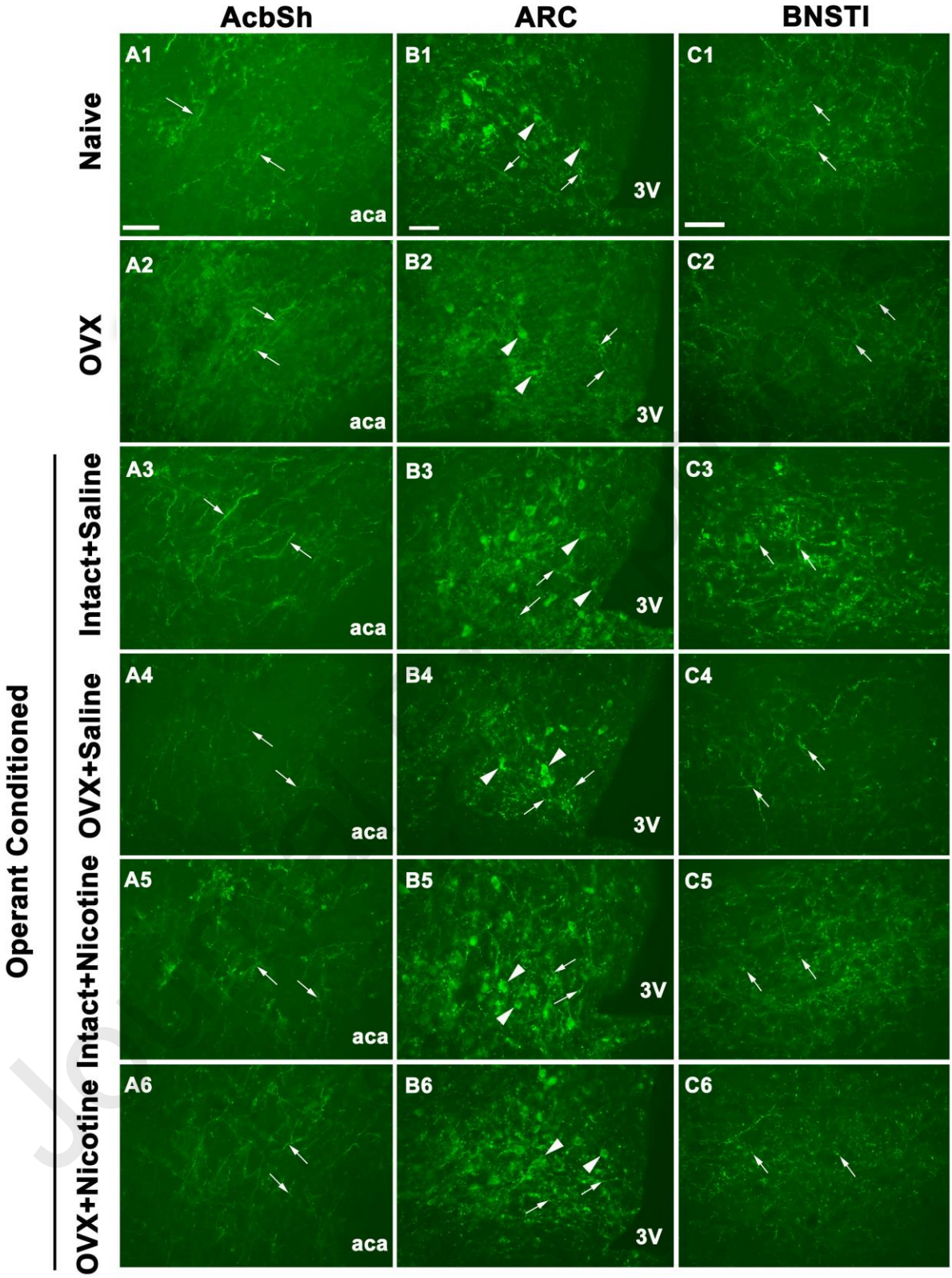
AcbSh
ARC
BNSTl
Naive
OVX
Operant Conditioned
Intact+Saline
OVX+Saline
Intact+Nicotine
OVX+Nicotine
A1
B1
C1
A2
B2
C2
A3
B3
C3
A4
B4
C4
A5
B5
C5
A6
B6
C6
aca
3V

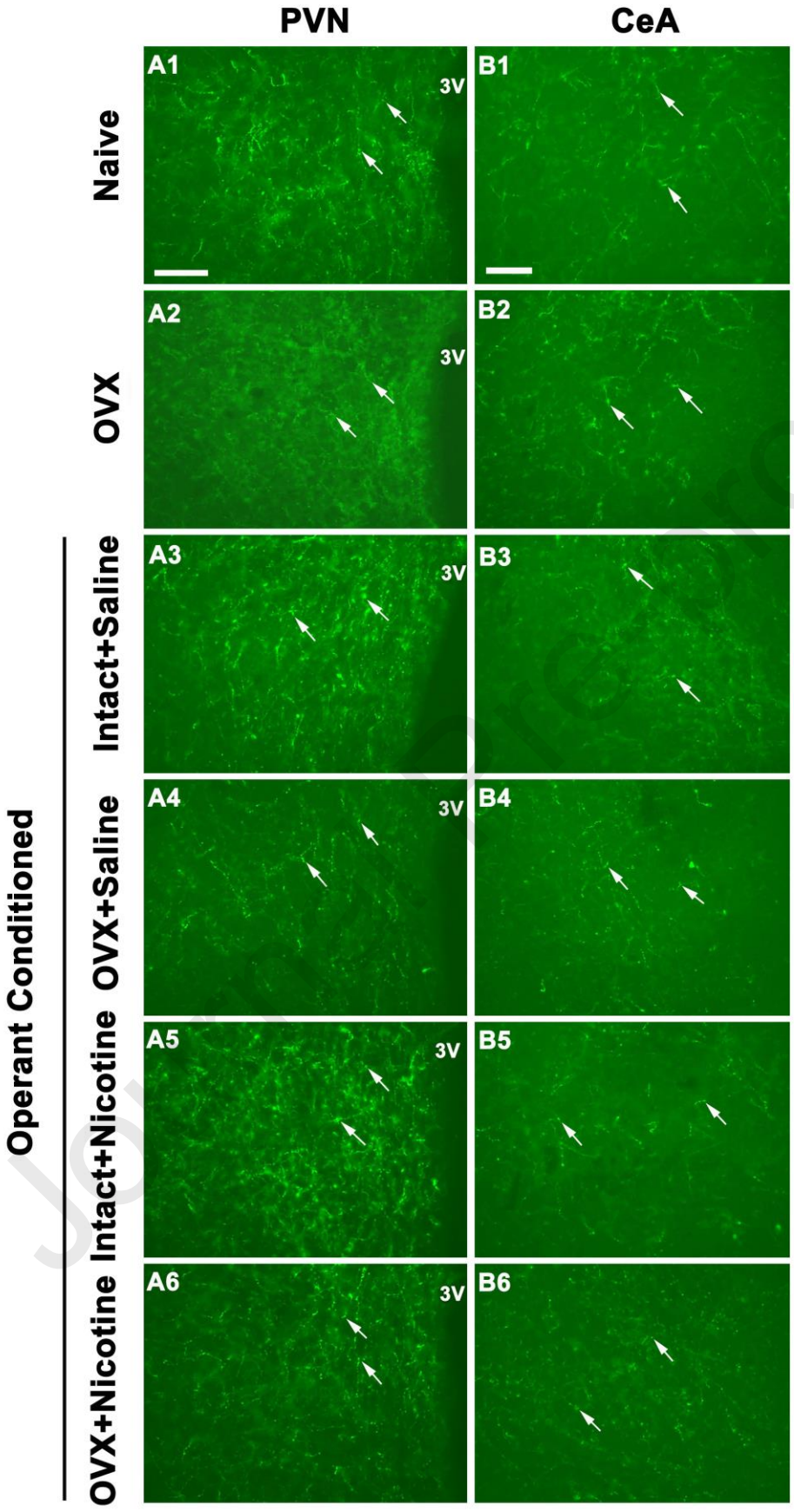
PVN
CeA
Naive
OVX
Intact+Saline
OVX+Saline
Intact+Nicotine
OVX+Nicotine
Operant Conditioned
A1
B1
A2
B2
A3
B3
A4
B4
A5
B5
A6
B6
3V

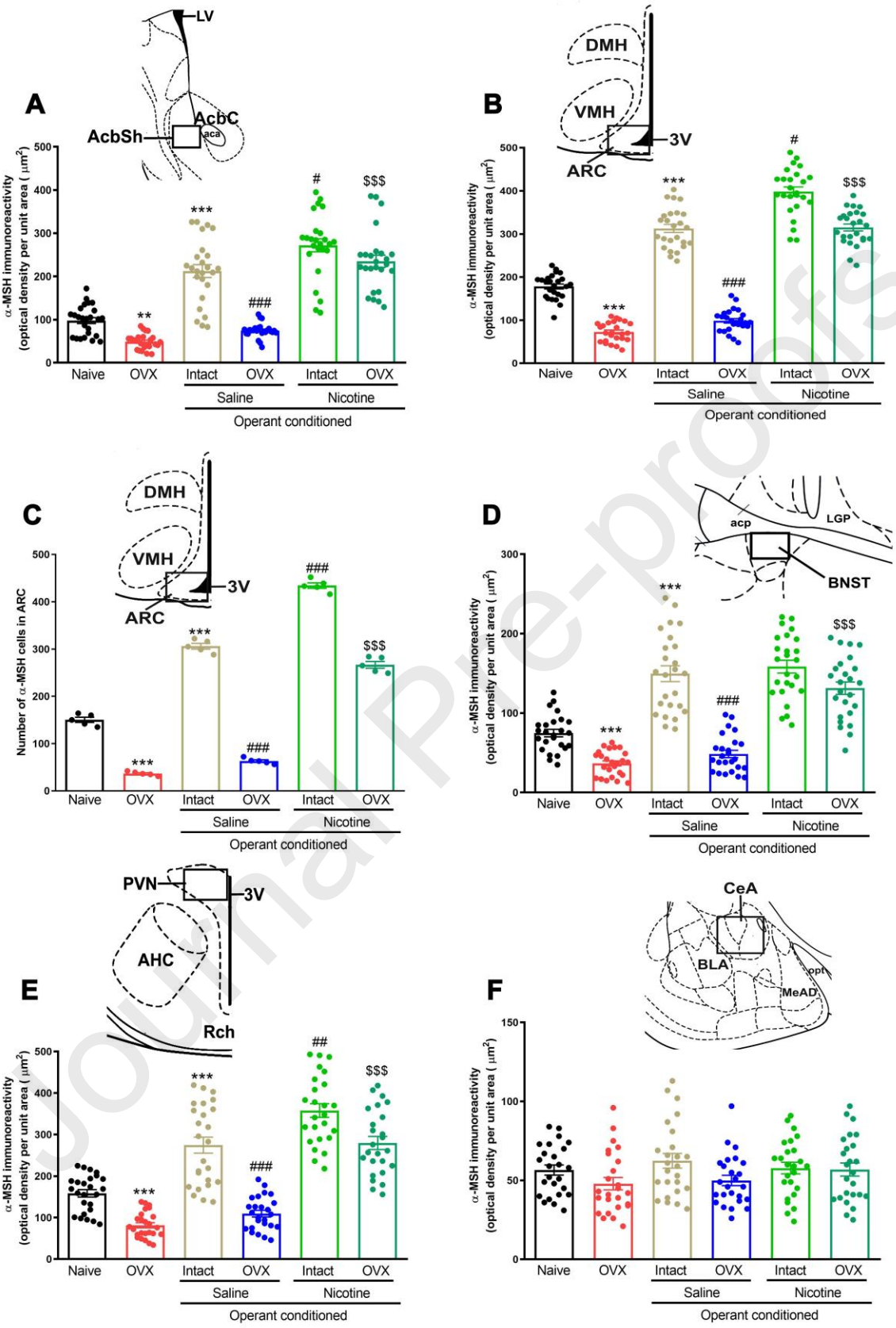

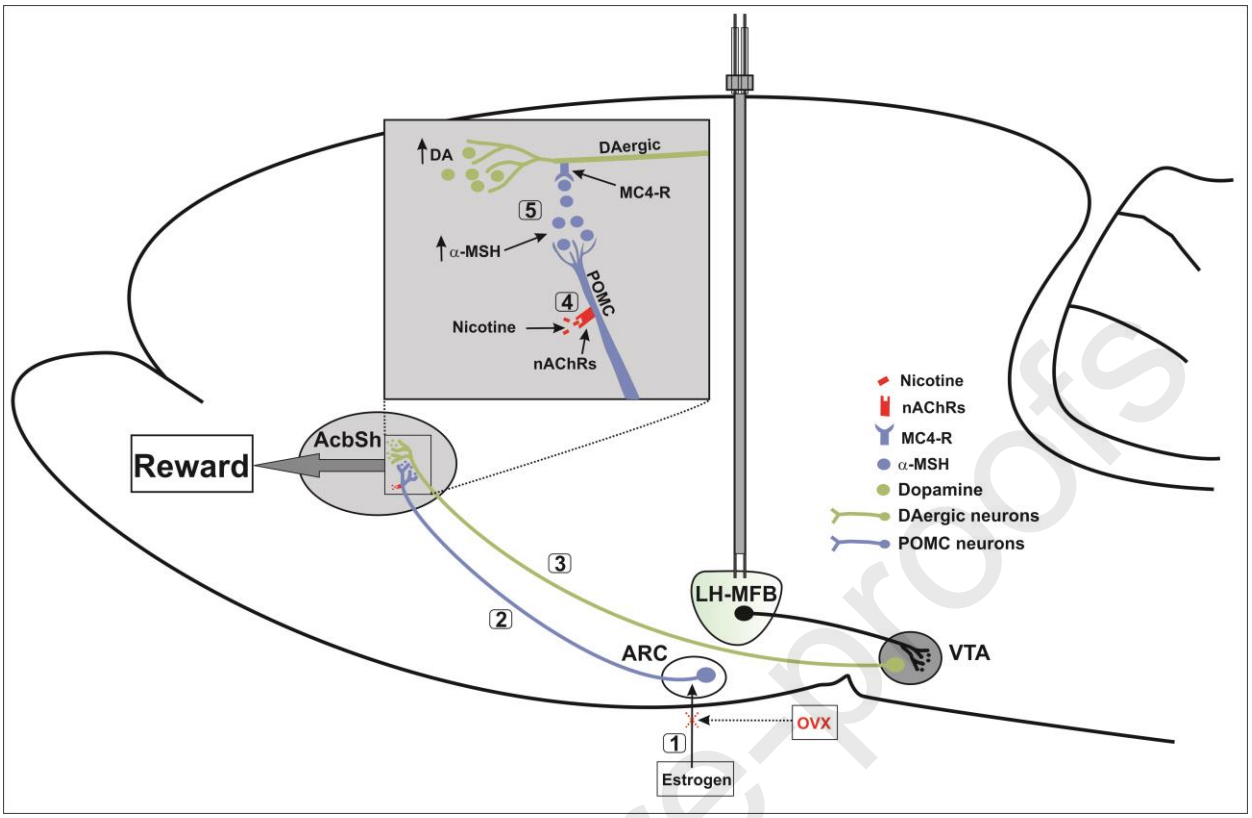

HIGHLIGHTS:

- The MC4-R mRNA level was increased in ipsilateral nucleus accumbens of the ICSS trained intact rats.
- Trained OVX rats revealed reward deficit behavior in ICSS paradigm.
- While Nicotine, α-MSH and NDP-MSH improved; HS014 impaired reward behavior.
- α-MSH or NDP-MSH potentiated nicotine reward however HS014 attenuated the same.
- α-MSH-ir was decreased in the reward processing regions in the OVX rats, while nicotine treatment restored the same.